Hungarian University of Agriculture and Life Sciences

EFFECTS OF LIGHTING ENVIRONMENTS AND OPTIMIZATION POSSIBILITIES

Dániel Szabó

Budapest

2026

Doctoral School: Doctoral School of Agricultural and Food Sciences

Discipline: Food sciences

Head of Doctoral School: Prof. Melinda Kovács DSc, MHAS

Supervisor: Prof. László Sipos PhD
Hungarian University of Agriculture and Life Sciences
Institute of Food Science and Technology
Department of Postharvest, Supply Chain, Commerce and Sensory Science

....

Approval of the Head of School Approval of Supervisor

1. Background

Light is one of the key environmental factors in life. The light conditions for outdoor crop production are basically determined by seasonal changes resulting from the Earth-Sun geometry and geographical position. The daily light integral (DLI) is the sum of the photon flux values measured per second over a square meter during a day, in the wavelength range of photosynthetically active radiation (400–700 nm). DLI maps show the spatial and temporal variations and distributions of DLI values. So far, only a few countries have published DLI maps (China, USA); our research group has prepared maps for Hungary, Spain, and Slovakia. DLI maps serve as a decision-making tool, providing an objective information base for analyzing the distribution of light available to plants at the regional level. The creation of DLI maps is a complex, slow, multi-step, and inefficient process. The manual collection of DLI values, which form the basis for mapping, takes orders of magnitude more time than if the same task were performed automatically. The efficiency and accuracy of the workflow should be improved through software development and automation, and supplemented with correction mechanisms, as the collected data is often burdened with inaccuracies.

Recently, fully enclosed cultivation facilities have made it possible to perfectly control the environmental parameters required by cultivated plants. In terms of light, factors such as light intensity and distribution, illumination duration and timing, spectral content, distance between light source and plant, and geometry can be controlled. Today, there is growing interest in light-emitting diode (LED) based lighting. LEDs convert energy into light more efficiently, emit light in a narrow spectral range (1–2 nm), generate relatively little heat, are easy to control, are becoming increasingly affordable, and their light parameters are easy to monitor. The equipment needed to measure LEDs and the light they emit is readily available. In plant cultivation practice, LEDs are integrated into panels. Due to the complexity of the system, even two identical light environments may differ in terms of the properties of the emitted photon flux that can be used by plants, therefore it is necessary to validate the light environments used in plant cultivation practice by instrumental measurement.

Light-specific treatments are also becoming increasingly important in post-harvest experiments. In this context, increasing the shelf life of freshly picked, commercially available vegetables and fruits is a desirable goal, which can potentially be achieved through light treatments. Since 54% of food waste in the EU is generated by households (Eurostat, 2022), this would also help combat food waste. The lighting environments of open fields, cultivation facilities, post-harvest storage, and research spaces are designed with plant light requirements in mind. In contrast, human light perception requires a completely different approach. Human vision is fundamentally determined by visual acuity, contrast sensitivity, and color vision, for which several medical sensory methods have been developed. During sensory testing, evaluators act as "measuring instruments," so their suitability is crucial during testing.

The most important criteria for standard color comparison are an evaluator with normal color vision, reproducible lighting and viewing geometry. However, if the basis for evaluation is not visual assessment, it is advisable to ensure that the color of the products does not influence the evaluators' decisions by designing the test conditions appropriately. This ensures that the assessor has no preconceptions about the product in terms of taste, smell, texture, or preference. For example, without masking, under standard white light (D65), reviewers will consider the yellower cooking oil to be more natural and contain more nutrients, the darker tea to have a more intense flavor, and the greener olive oil to be fresher, even before tasting and smelling, which can lead to biased evaluations. For this reason, it is necessary to reduce the intensity or quality of color perception, but it is advisable to mask or conceal it. In the sensory laboratories of food production plants, it is necessary to perform sensory tests on production batches on a daily basis, However, to my knowledge, there is no suitable method available for the visual sensory masking of sunflower and rapeseed oils, as well as blended cooking oils made from these two plants, and this also applies to the product group of green and black tea infusions.

2. Objectives of the work

The main goal of my dissertation is a complex evaluation of the effects and optimization possibilities of light environments. On the one hand, the photosynthetically usable light reaching field plants, on the other hand, the validation and evaluation of the effects of light environments that can be implemented in a climate chamber for harvested plants, and on the third hand, the adjustment and adaptation of light environment masking and masking with colored test glasses for sensory testing.

I present the objectives of the research divided into the following sub-objectives.

- Creation of DLI maps of Portugal in multiple resolutions and summarizing and comparison of the temporal and spatial patterns of DLI value distributions in Portugal.
- Automate the data collection workflow of DLI mapping and develop an efficient, database-based, self-healing software with increased reliability, increased automation, and reduced supervision requirements.
- Comparison of the photon flux density distributions of two identically designed chambers of a two-chamber climate chamber, as well as determination of the dependence of the photon flux density of the LED panel used in the climate chamber on distance and the extent of the decrease in photon flux density towards the edges.
- Determination of the temporal evolution of chlorophyll content in lettuce leaves of the *Lactuca sativa* 'Casey' variety under different light environments.
- Creating masking light environments in an LED light cabin developed for sensory testing to conceal slight color differences in green and black tea infusions made from fermented leaves of tea (*Camellia sinensis* L.) from different origins. In connection with this, my goal is to:
  - determination of spectral properties of green and black tea infusions in CIELAB color space,
  - testing the vision of sensory evaluators,
  - determination of visual differences between green and black tea infusions under standard white light source (D65) and under masking illumination, and evaluation of the masking effect.
- Testing the masking effect of colored (cobalt blue) standard test cups developed for olive oils on sunflower oils, rapeseed oils, and edible oils made from a blend of these two plants. In connection with this, my goal is to:
  - determination of spectral properties of sunflower oils, rapeseed oils, and mixed edible oils in the CIELAB color space;
  - spectral characterization of a standardized test cup (cobalt blue) developed for olive oils;
  - testing the vision of sensory evaluators (color vision accuracy, color discrimination ability, contrast sensitivity);
  - determination of visual differences between sunflower, rapeseed, and blended edible oils under a standard white light source (D65) in a transparent olive oil testing cup and under a standard white light source (D65) in a colored (cobalt blue) olive oil testing cup. My goal is to evaluate the masking effect.

3. Materials and methods

3.1. Daily light integral mapping

3.1.1. Material: continental Portugal

The continental territory of Portugal is located in southwestern Europe, on the Iberian Peninsula. The following data refer only to this territory, i.e. excluding the islands belonging to the country (the Azores and Madeira). It covers an area of 89,015 km^2, between 36 and 42 degrees north latitude and 6 and 9 degrees west longitude. Its terrain is relatively varied, with the following proportions of areas at different altitudes: 0–200 m 40–45%, 200–600 m 25–30%, 600–1200 m 15–20%, 1200–2000 m 5–7%, above 2000 m <1%. Portugal has many agricultural regions characterized by diverse climatic conditions, soil types, topographical features, and different crops. The agricultural regions of the mainland are divided between coastal (Co) and inland (In) areas, and into northern (N), central (C), and southern (S) regions:

- north (N): Entre Douro e Minho (Co–N), Trás os Montes (In–N)
- center (C): Beira Litoral (Co–C), B. Alta (In–C), B. Baixa (In–C), Ribatejo e Oeste (Co–C)
- south (S): Alentejo (Co–S, In–S), Algarve (Co–S) (Fraga & Santos, 2021, Pereira *et al.*, 2021)

3.1.2. Method: partially automated DLI mapping workflow and calculations

I automatically request the values needed for DLI mapping by repeatedly calling a remote server (dli.suntrackertech.com) capable of providing DLI values using a PHP script. The remote server expects geocoordinate pairs (longitude, latitude), and we save the monthly average DLI values from the response to the corresponding empty fields in the database for the twelve months of the year. The geocoordinate pairs sent during the request are based on a 30×30 meter resolution grid, which is derived from NASA's SRTM 1 arc second resolution digital elevation model. The process is carried out with the permission of the remote server operator, SunTracker Technologies Ltd. of Canada, taking care to keep the load within acceptable limits. The script runs again if there are formally incorrect or empty fields in the database and only stops when all database fields are properly filled. The data obtained was used to create DLI maps with resolutions of 2 $mol \cdot m^{-2} \cdot d^{-1}$ and 5 $mol \cdot m^{-2} \cdot d^{-1}$.

3.2. Light validation of climate chamber

3.2.1. Material: light panel, photosynthetic light flux measurement, photosynthetic light flux distribution

The study was conducted in two identical test chambers of a two-compartment plant growth chamber, in which the environmental parameters of light, temperature, and humidity can be controlled. Lighting is provided by two Ledium Black Sparkle Modular64 Base LED panels, one per chamber. Its main components are: a heat sink, a printed circuit board, Luxeon SunPlus 2835 LEDs (full spectrum, but with increased intensity at chlorophyll absorption maxima), and a polycarbonate optical lens. The lighting system also includes a power supply, control unit, and connecting cables.

3.2.2. Method: climate chamber with three cultivation surfaces, measurement of grid points on the cultivation surface

I characterized the surface of the lower three levels of the left and right chambers of the experimental climate chamber by measuring the extended photosynthetic light flux (400–750 nm) at the following light source–level distances: upper 155 mm, middle 245 mm, lower 335 mm (Figure 1).

Figure 1. Measurement grid points applied to horizontal surfaces on the upper, middle, and lower levels of the right chamber of the climate chamber illuminated by the Ledium Black Sparkle Modular64 Base (own photo)

Calibration table layout: 3×3 cm matrix, 6 columns, 11 rows = 66 grid points. The grid points are numbered from 1 to 66 in ascending order from left to right. I started the measurements 10 minutes after turning on the light source to ensure the thermal stability of the LEDs. In the left and right test areas, I measured the photosynthetic photon flux using an Apogee Instruments DLI–600 instrument developed for point measurements in the 400–750 nm wavelength range, with 100 measurements per grid point. I used the Kruskal–Wallis test for the statistical evaluation of the light flux values obtained, and the Dunn test with Bonferroni correction for pairwise comparisons. I visualized the results using MATLAB R2025b software (distribution and contour plots).

3.3. Stimulating chlorophyll production in lettuce using LED lighting

3.3.1. Material: species, species type, variety

In my tests, I used individual specimens of the 'Casey' variety (*Lactuca sativa* 'Casey'), which belongs to the butterhead lettuce variety group. The lettuces were grown in Poland, in a greenhouse, under pesticide-free conditions, and were available in retail stores with roots, wrapped in plastic film. I tried to ensure that the specimens came from the same production batch.

3.3.2. Method: climate chamber, light programs (10 minutes of light, 10 minutes of darkness), temperature 4°C, relative humidity 70%, 14 days

The roots of the lettuce were kept in 2 cm of water throughout the 14 days of the experiment, which I checked daily and topped up as necessary. During the research, I examined the effect of two different lighting environments on the chlorophyll content of lettuce. My goal was to compare the effect of lighting on chlorophyll production in a dark, closed storage room without lighting and in an LED-based lighting environment optimized for chlorophyll production. I conducted my research in an LED-lit climate chamber, in an environment that was presumed to stimulate chlorophyll production. The experimental settings were as follows: photosynthetic photon flux 128 $\mu mol \cdot s^{-1}$ between 400 and 750 nm, light program 10 minutes of light / 10 minutes of darkness, temperature 4°C, relative humidity 70% (Figure 2).

Figure 2. *Lactuca sativa* 'Casey' variety in an LED-illuminated climate chamber (own photo)

I determined the total chlorophyll content using an Apogee Instruments MC–100 handheld meter. I took measurements using a standard measurement circle diameter of 9 mm on the uppermost part of one outer and one inner leaf of the lettuce, in both cases taking 5 measurements to the right of the main vein and 5 measurements to the left of the main vein. I started the experiment at 10 a.m. on the first day, so I performed the measurements at 10 a.m. every day to avoid distorting my results with errors resulting from changes in the measurement time. I performed the statistical evaluations using the non-parametric Kruskal–Wallis test, while the pairwise comparisons were performed using Dunn's non-parametric test with XLSTAT software.

3.4. Color masking of green and black tea samples of different origins

3.4.1. Material: green and black tea (*Camellia sinensis* L.) samples

When selecting the test samples, my aim was to ensure that the major tea-producing countries and tea-growing regions were represented in proportion to their importance (Table 1, Table 2).

Table 1. Green tea samples included in the study

#	Green tea name	Country	Province
1.	Fukamushi Sencha	Japan	Uji
2.	Gyokuro Jikagise	Japan	Uji
3.	Gyokuroh Gokoh	Japan	Uji
4.	Gyokuro Karigane	Japan	Uji
5.	Sencha Shiruki	Japan	Uji
6.	Matcha Jikagise	Japan	Uji
7.	Mengding Ganlu	China	Sichuan
8.	Xihu Longjing	China	Zhejiang
9.	Formosa Bi Luo Chun	Taiwan	Unknown
10.	Gaba Green	Taiwan	Unknown
11.	Tien Shan Maojian	China	Jianshu
12.	Lu Shan Yun Wu	China	Jianshu
13.	Yunnan Bi Luo Chun	China	Yunnan
14.	Green Jade	China	Fujian
15.	Qing Zhen	China	Yunnan

Table 2. Black tea samples included in the study

#	Black tea name	Country	Province
1.	Gaba Black	Taiwan	–
2.	Jin Xuan Black	Taiwan	–
3.	Alishan Black	Taiwan	–
4.	Assam Black	Taiwan	–
5.	Fuliang Red	China	Fujian
6.	Yixing Red	China	Jianshu
7.	Bai Un Gongfu	China	Fujian
8.	Lapsang Souchong	China	Fujian
9.	DaYaYin	China	Yunnan
10.	Simao Golden thread	China	Yunnan
11.	Yongde Old wood red	China	Yunnan
12.	Golden Monkey	China	Fujian
13.	Darjeeling Monipur Assam	India	Assam
14.	Darjeeling Tinderet	Kenya	Tinderet
15.	Himalaya Darjeeling	India	Himalaya
16.	Nuwara Eliya	Sri Lanka	Nuwara Eliya
17.	Uva Highlands Uva Pekoe	Sri Lanka	Uva Highlands
18.	Darjeeling Naaibaizi	India	Naaibaizi
19.	Sri Lanka Pettyagalla	Sri Lanka	Pettyagalla
20.	Assam Golden leaf (blend)	India	Assam

3.4.2. Instrumental method: spectral characterization of team samples

I prepared a decoction from the green and black tea leaves included in the study in accordance with standard specifications. I poured 140 ml of freshly boiled water at 100°C over 2.8 g of tea leaves in a standard-sized small teacup, which I covered with a standard lid. I steeped the green tea leaves for 5 minutes and the black tea leaves for 6 minutes, then pipetted the resulting infusion into a cuvette and covered it with a cuvette cover. For the transmission measurements of the tea samples, I used disposable, standard (4-sided transparent polystyrene, 340–800 nm) 5 ml cuvettes with a 10 mm light path and a height of 45 mm (Figure 3). For spectral characterization of green and black tea infusions, I recorded the transmission of the infusions in the cuvettes in the visible wavelength range of 380–780 nm, with a resolution of 5 nm and a wavelength accuracy of ±0.5 nm, using an AOE Instruments UV–1600 spectrometer (Figure 4). For the spectrophotometric measurements, I prepared five parallel samples from each sample. I evaluated the teas considering the transmission factor of the cuvette.

Figure 3. Single-use polystyrene cuvette (own photo)

Figure 4. AOE Instruments (Shanghai) UV–1600 spectrometer (I1)

3.4.3. Sensory method: color vision tests by sensory evaluators, sensory tests of team samples under standard and light-masked conditions

As a first step, I tested the color vision of the evaluators so that only those with normal vision would participate in the sensory examination later. For this purpose, I used the pseudo-isochromatic Ishihara test (Figure 5), developed to identify color blindness, and the Farnsworth–Munsell 100 test (Figure 6), suitable for testing color hue discrimination ability, under the standard white light (D65) illumination of the Pantone Color Viewing Light BASIC 3 light booth (Figure 7) manufactured by JUST Normlicht GmbH.

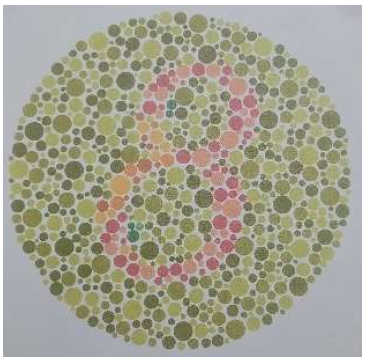

Figure 5. Ishihara color test chart (own photo)

Figure 6. Farnsworth–Munsell 100 hue discrimination test, in a light booth, under D65 white illumination (own photo)

I conducted the visual tests of the testers involved in the study and the product tests of the tea infusions in a standard D65 lighting environment, using a 0°/45° test geometry, which ensures that the light falls perpendicularly on the sample and the evaluator views the sample from a 45° angle. For the test, I used the Pantone Color Viewing Light booth and its D65 mode. The device's internal test space ensures comfortable sensory testing (640×330×360

mm). In the second step, I conducted sensory tests under standard lighting and testing conditions. I prepared the tea infusions in the standard manner and poured them into standard tea testing cups (ISO 3103:2019) (Figure 8). I performed the visual tests of the testers involved in the study and the product tests of the tea infusions in a standard D65 lighting environment with a 0°/45° test geometry, which ensures that the light falls perpendicularly on the sample and the evaluator views the sample at a 45° angle. For the test, I used the Pantone Color Viewing Light light booth and its D65 mode. The device's internal test space ensures comfortable sensory testing (640×330×360 mm). In the second step, I conducted sensory tests under standard lighting and testing conditions. I prepared the tea infusions in the standard manner and poured them into standard tea testing cups (ISO 3103:2019) (Figure 8).

Figure 7. Just Normlicht Pantone Color Viewing Light BASIC 3 light booth (own photo)

Figure 8. Standard tea brewer and tea tasting cup (own photo)

For sensory testing, I used a standard difference test method, the triangle test. The evaluators had to select the different sample from a set of three tea infusions containing two identical samples and one different sample and justify their choice. I performed sensory comparisons of the tea infusions in a standard light booth (Pantone Color Viewing Light, D65). I recorded the results and evaluated them according to the relevant standard, based on the binomial theorem and the sequential procedure (ISO 4120:2021, ISO 16820:2019). In the third step, I set up different lighting conditions in a spectrally tunable LED light cabin and examined their masking effect using the triangle test method. The spectrally tunable LED light cabin (BME, MOGI), designed for examining lighting environments, contains five LED light sources with different peak wavelengths: red (640 nm), green (530 nm), blue (460 nm), amber (590 nm), and neutral white. The intensity of each LED channel can be adjusted between 0 and 255. The LEDs are located on four fixed panels in a 1.5×1×1 meter cabin (Figure 9).

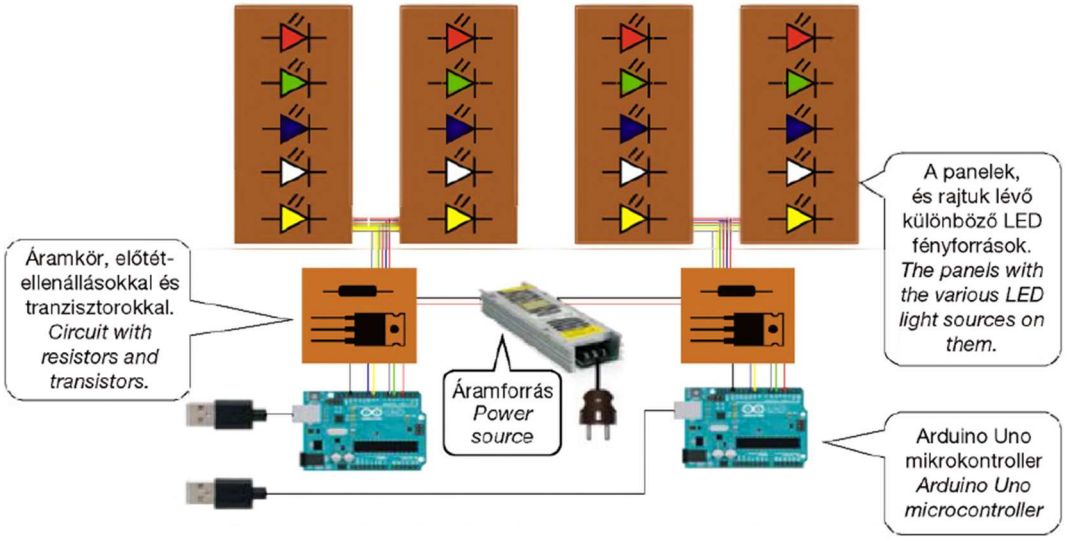

Figure 9. Schematic structure of a spectrally tunable measuring station (Dominek, 2017)

I used five different settings for green and four different settings for black tea infusions (Table 3).

Table 3. Masking light settings (0–255) applied to green and black tea infusions

Masking light settings for green tea decoctions (0–255)					
Settings	**Red**	**Green**	**Blue**	**White**	**Amber**
1. setting	110	0	0	0	160
2. setting	255	0	0	0	45
3. setting	155	0	55	0	65
4. setting	205	25	25	0	0
5. setting	90	120	230	255	90
Masking light settings for black tea infusions (0–255)					
1. setting	255	0	0	0	0
2. setting	0	255	0	0	0
3. setting	0	0	255	0	0
4. setting	0	0	0	0	255

3.5. Testing the masking effect of standard test cups (cobalt blue) developed for olive oils on sunflower oils, rapeseed oils, and mixed edible oils

3.5.1. Ingredients: sunflower oils, rapeseed oils, mixed edible oils

I tried to obtain sunflower and rapeseed oils, as well as mixed cooking oils, from as wide a range of sources as possible for the study. Their list is shown in tabular form below (Table 4).

Table 4. Sunflower oil, rapeseed oil, and mixed oil samples included in the study (listed in alphabetical order by commercial name)

No.	Trade name	Plant source	Composition
1.	Auchan	sunflower	Refined sunflower
2.	Bellasan	sunflower	Refined sunflower
3.	Floriol Active	rapeseed	Refined rapeseed
4.	Floriol Omega+	rapeseed+napraforgó	Refined rapeseed (70%) and high oleic sunflower (30%)
5.	Huile de Colza (Auchan budget)	rapeseed	100% refined rapeseed
6.	Kunsági éden	sunflower	100% refined sunflower oil
7.	Kunsági éden Szuper	sunflower+rapeseed	70% refined sunflower oil, 15% refined rapeseed oil, 15% refined sunflower oil with high oleic acid content
8.	Natur Organic 100% hidegen sajtolt	sunflower	100% cold, pressed from hulled seeds sunflower
9.	Rapso	rapeseed	100% refined rapeseed
10.	S-Budget	sunflower	100% refined sunflower
11.	Tanya Aranya Grande	sunflower	100% refined sunflower
12.	Tesco	sunflower	100% refined sunflower
13.	Vénusz Sütőolaj	sunflower	First-pressed sunflower seeds (85%), sunflower seeds with high oleic acid content (15%)
14.	Vénusz Omega	rapeseed+sunflower	Refined rapeseed (60%), first-pressed refined sunflower (40%)
15.	Vénusz 100% első préselésű finomított	sunflower	100% first-pressed refined sunflower oil
16.	Vita D'or	sunflower	Sunflower

3.5.2. Instrumental method: spectral characterization of masking cups and cooking oil samples

For spectral characterization of the olive oil test cups, I determined the spectral transmission of cobalt blue and transparent cups in the 380–780 nm (visible) wavelength range with a resolution of 1 nm. For the transmission

measurements of the edible oil samples, I used disposable, standard (4-sided transparent, polystyrene, 340–800 nm) cuvettes with a 10 mm light path, 45 mm height, and 5 ml capacity. For the spectral characterization of the cooking oils, I recorded the spectral transmission values in the wavelength range of 380–780 nm, with a resolution of 5 nm. The measurements were performed using an AOE Instruments UV–1600 spectrometer with an accuracy of ±0.5 nm. I determined the CIELAB color space coordinates from the transmission spectra (L*, a*, b*, C^*_{ab}, h^*_{ab}, ΔE^*_{ab}).

2.5.3. Sensory method: color vision tests by sensory evaluators, sensory test under standard conditions and in colored cups (triangle test)

I conducted the sensory evaluators' color vision tests (pseudo-isochromatic Ishihara test, Farnsworth–Munsell 100 hue difference test) as described and under the conditions specified for tea infusions. The novelty of the sensory testing of edible oils is that we adapted the standard, colored (cobalt blue) olive oil testing cup and standard olive oil warmer used in international olive oil testing to sunflower oils, rapeseed oils, and their blends. During the sensory testing, I used standard material and colored (cobalt blue) cups: stable, heatable base, narrowing towards the mouth, base-less glass container, homogeneous glass, dark, colored material (Figure 10).

Figure 10. Standard cobalt blue olive oil testing cup (ISO 16657:2023) (own photo)

I used watch glass to prevent oil oxidation and contamination. In accordance with standard specifications, I tempered the oil samples (28–30°C) using a device specially designed for this purpose (IOC, 2018, 2020a, ISO 16657:2023) (Figure 11).

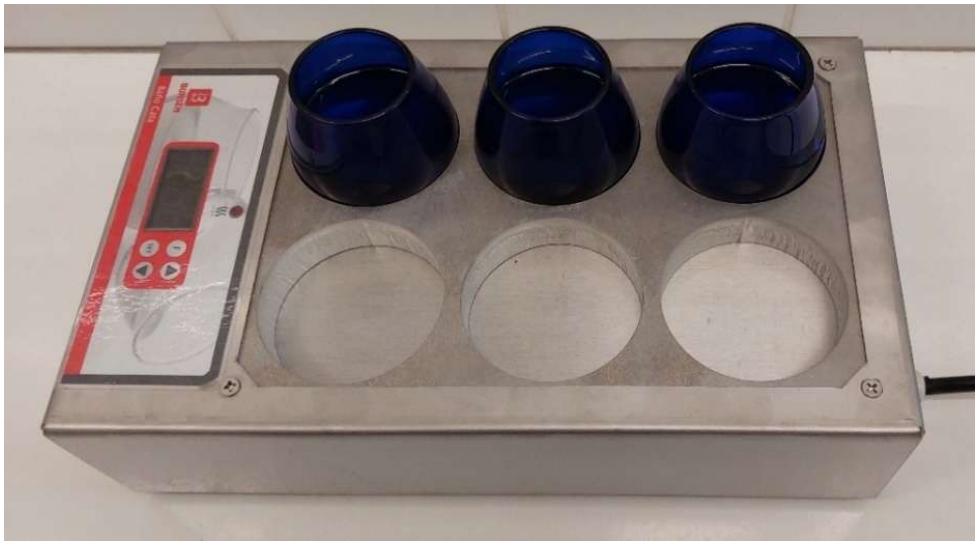

Figure 11. Standard olive oil heating device (ISO 16657:2023) (own photo)

4. Results and discussion

4.1. Daily light integral calculations and Portugal DLI map

For the first time, maps showing monthly average DLI values were prepared for continental Portugal, with resolutions of 2 mol·m^{-2}·d^{-1} and 5 mol·m^{-2}·d^{-1} (Figure 12).

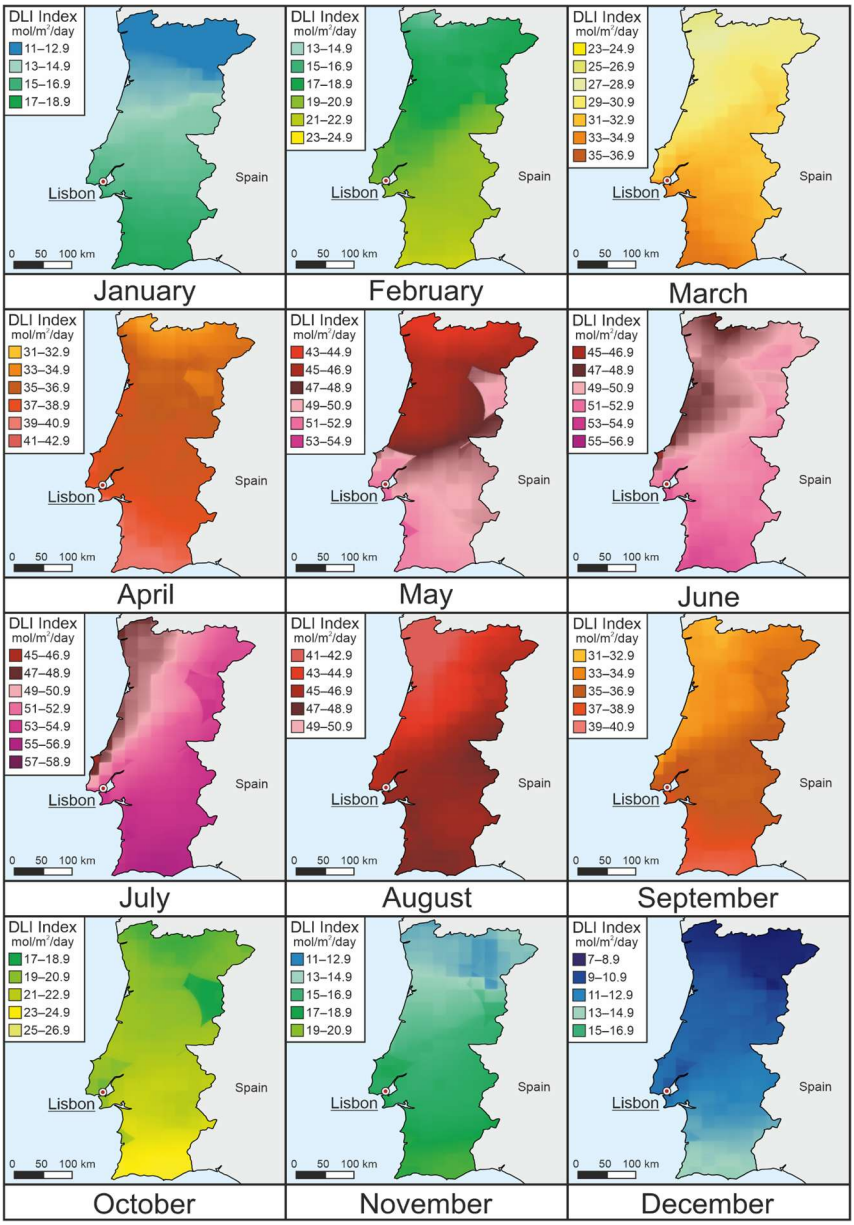

Figure 12. Monthly DLI maps for Portugal with a resolution of 2 mol·m^{-2}·d^{-1}, which is a typical representation scale used to compare local differences in regional dimensions. The distribution of meteorological stations used for DLI calculations is not homogeneous, which causes certain visualization difficulties, especially in central regions. (On the scale, the "from" and "to" values end with two digits, but for practical reasons they have been shortened to one decimal place.)

4.1.1. Regional differences

The DLI value is basically determined by geographical position and seasonal changes resulting from the Sun-Earth geometry, but it is also influenced by several other factors (e.g., weather conditions, topographical and horizontal effects, vegetation, geological formations). My results confirm that DLI values in Portugal increase from north to south, with the mountains in the northern part of the country causing significant orographic precipitation (increasing cloud cover), thereby reducing DLI values. The proximity of the coastline moderates the intensity of the DLI-reducing effect of the mountains, in contrast to the more inland mountainous regions, where this phenomenon is hardly observable. The N-S gradient has a stronger influence on the national trend in DLI values than local conditions.

4.1.2. Seasonal fluctuations

DLI values show a characteristic pattern every month. The lowest values occur in the winter months, dynamic growth is typical in the spring months, and the highest values occur in the summer months. The highest DLI values are in July (45–59 $mol \cdot m^{-2} \cdot d^{-1}$). In autumn, DLI values decrease dynamically until they reach their lowest values in December (7–17 $mol \cdot m^{-2} \cdot d^{-1}$). The width of the monthly DLI value ranges (the differences between the minimum and maximum values for a given month) is similar, but there are smaller seasonal variations. These ranges are generally narrower in the winter months (January: 8 $mol \cdot m^{-2} \cdot d^{-1}$) and wider in the spring and summer months (March, July: 14 $mol \cdot m^{-2} \cdot d^{-1}$). They narrow again during autumn (11 $mol \cdot m^{-2} \cdot d^{-1}$), while the narrowest range is characteristic of January values (8 $mol \cdot m^{-2} \cdot d^{-1}$). The largest monthly fluctuations in DLI values are observed in summer.

4.1.3. Summary assessment

Portugal has a characteristic north-south geographical zonality, resulting in a clearly recognizable gradient with topographical modifying factors. Topography influences cloud cover, precipitation, and hours of sunshine. DLI values reflect the north-south gradient, coastal and inland effects, and orographic characteristics. Beyond topographic factors, Mediterranean seasonal DLI patterns can be characterized by their values, ranges, and distribution. In Portugal, the north-south DLI gradient is dominant, but other factors should not be ignored when assessing local conditions. A map with a resolution of 2 $mol \cdot m^{-2} \cdot d^{-1}$ is suitable for showing such differences. Due to the regional scale, it is also advisable to produce maps with a resolution of 5 $mol \cdot m^{-2} \cdot d^{-1}$, as these can be easily compared with previous DLI maps of larger countries and continents.

4.2. Automation of daily light integral (DLI) data collection, new developments

I had previously developed a method for automating the collection of DLI data, which is essential for mapping Hungary's DLI, and further refined it during the collection of DLI data for Portugal. When creating Portugal's DLI map, I implemented the automation process with the following new developments and efficiency-enhancing solutions. I made it possible to run the script in a Windows environment as well as Linux, which was necessary to increase the number of participating computers. This allowed me to collect more DLI values per unit of time. Instead of saving to a CSV file, I developed a faster, more efficient, and easier-to-check database-based storage method (MySQL). In the event of a lack of response from the remote server or a formal error, the relevant database field remains empty, which is corrected by the script's self-correcting mechanism, which jumps to the beginning of the database and runs repeatedly. To avoid overloading the remote server, I inserted a two-second delay between each request, which was necessary because the remote server allows a maximum of thirty requests per minute from a network, thus ensuring the continuity of data retrieval. All of this has increased the reliability of data collection, increased the level of automation, and reduced the need for supervision.

4.3. Light validation of climate chamber

My results confirmed that the homogeneity of the extended photosynthetic light flux density (400–750 nm) distribution on the test surface increases with increasing distance from the light source (upper level 155 mm, middle level 245 mm, lower level 335 mm). The further away we are from the light source, the more homogeneous the light flux distribution. The measurements were taken in the left and right chambers of the climate chamber using the same LED light source, the same settings, the same light source-sample geometry, and the same light reflection environment. The extended photosynthetic light flux density values measured in the left chamber are comparable to those measured in the right chamber. My results confirm that the extended photosynthetic light flux density values were significantly different at the same light source-level distance and at the same grid point. To make the results easier to interpret, I prepared contour plots supporting this finding on an absolute scale in terms of extended photosynthetic light flux density (400–750 nm) ($\mu mol \cdot m^{-2} \cdot s^{-1}$) and on a relative scale (%) (Figure 13).

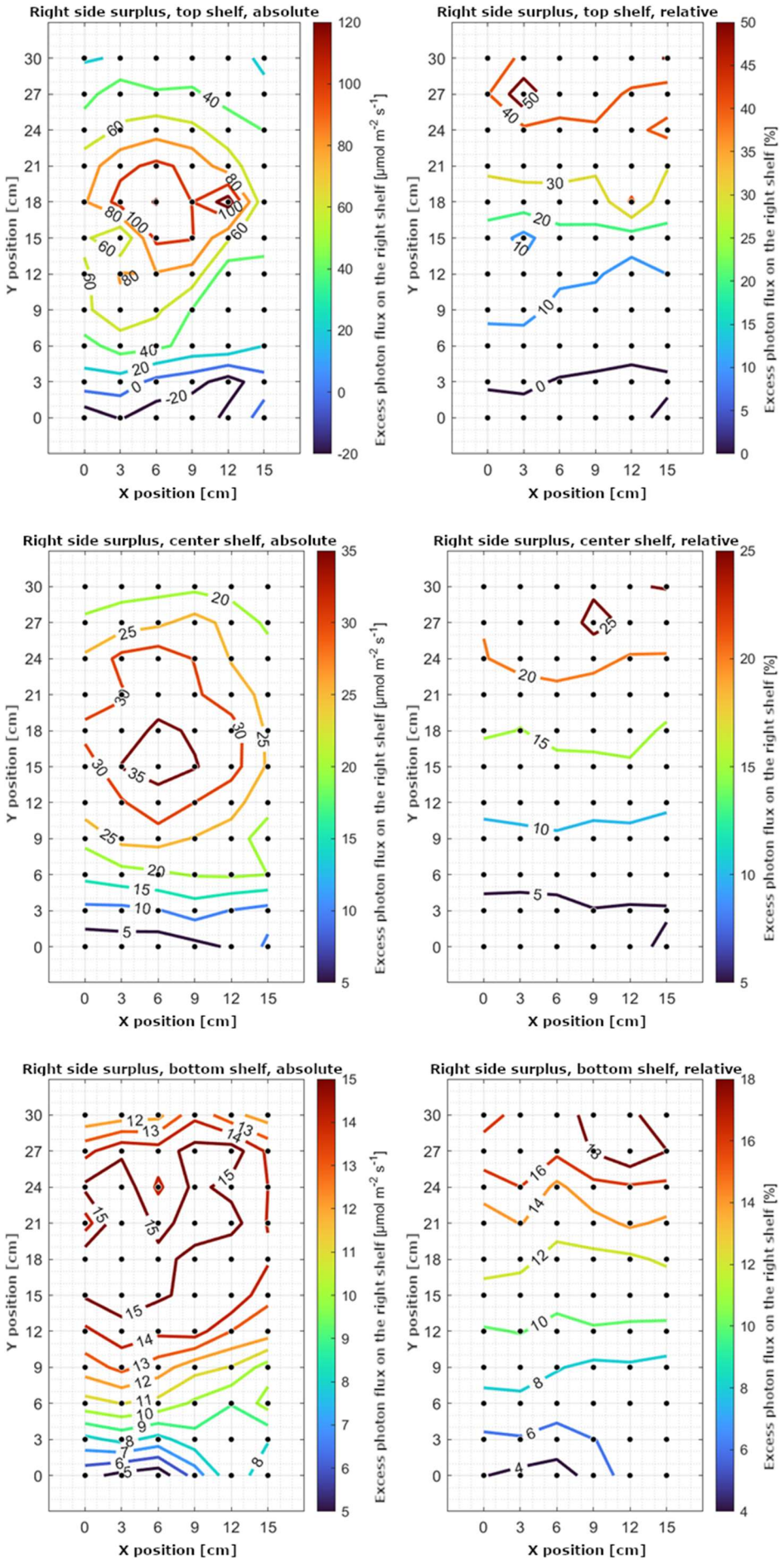

Figure 13. Absolute values (µmol·m^{-2}·s^{-1}) and relative values (%) of the difference in the extended photosynthetic photon flux density (400–750 nm) values of the dot grids of the climate chamber upper left–upper right, middle left–middle right, and bottom left–bottom right levels

4.4. Stimulating chlorophyll production in lettuce using LED lighting

The results related to the development of chlorophyll production in lettuce are presented in the following structure. In the first step, I present the development of chlorophyll content measured on the outer leaves of lettuce treated with light and kept in the dark from 1 to 14 days. In the second step, I present the development of chlorophyll content measured on the inner leaves of lettuce treated with light and kept in the dark from 1 to 14 days. The Kruskal–Wallis test performed based on the descriptive statistics of the measurements for the samples (number of measurements, minimum value, maximum value, mean, standard deviation) was significant, since the calculated probability value was smaller than the originally chosen significance level ($\alpha = 0.05$). Due to the significance of the Kruskal–Wallis test, I further analyzed the samples with a multiple pairwise comparison test, Dunn's post hoc test. Based on this, the result of the test can be stated that the outer leaf of the lettuce treated with light showed a significantly higher value than the outer leaf of the lettuce kept in the dark from the 9th day onwards. The experiment lasted for 14 days, the temperature in the chamber was set to 4°C. I also present the change in chlorophyll content of the two outer leaves tested (light treatment/dark) in a bar graph. I have marked the chlorophyll values of the lettuce leaves treated with light in green, and the chlorophyll values of the lettuce leaves kept in the dark in gray. From the figure, it can be stated that while the chlorophyll content of the lettuce leaves treated with light increases slightly or stagnates, the chlorophyll content of the lettuce leaves kept in the dark continuously decreases during the tested period (Figure 14).

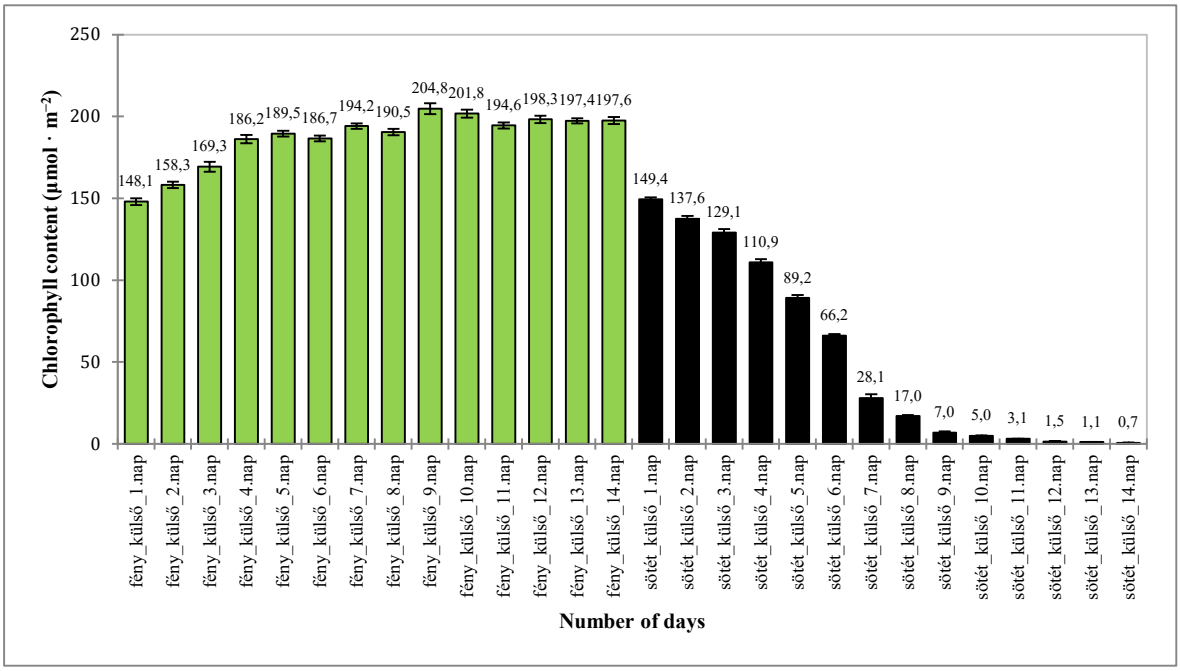

Figure 14. Changes in chlorophyll content in outer leaf of lettuce, with light treatment and in the dark, at 4°C

In the second step, I present the development of chlorophyll content measured on the inner leaves of light-treated and dark-treated lettuce from 1 to 14 days. The Kruskal–Wallis test performed in the knowledge of the descriptive statistics of the measurements for the samples was significant, since the calculated probability value was smaller than the chosen significance level ($\alpha = 0,05$). Due to the significance of the Kruskal–Wallis test, I further analyzed the samples with Dunn's post hoc test. Based on this, it can be stated as the result of the test that the inner leaves of the light-treated lettuce showed a continuously significantly higher value than the inner leaves of the lettuce kept in the dark from the 9th day onwards. The experiment lasted for 14 days, the temperature in the chamber was set to 4°C. I also present the change in chlorophyll content of the two inner leaves examined (light treatment/dark) in a bar graph. I have marked the chlorophyll values of the lettuce leaves treated with light in green, and the chlorophyll values of the lettuce leaves kept in the dark in gray. It can be seen from the figure that while the chlorophyll content of the lettuce leaves treated with light increases slightly or stagnates, the chlorophyll content of the lettuce leaves kept in the dark continuously decreases during the examined period (Figure 15).

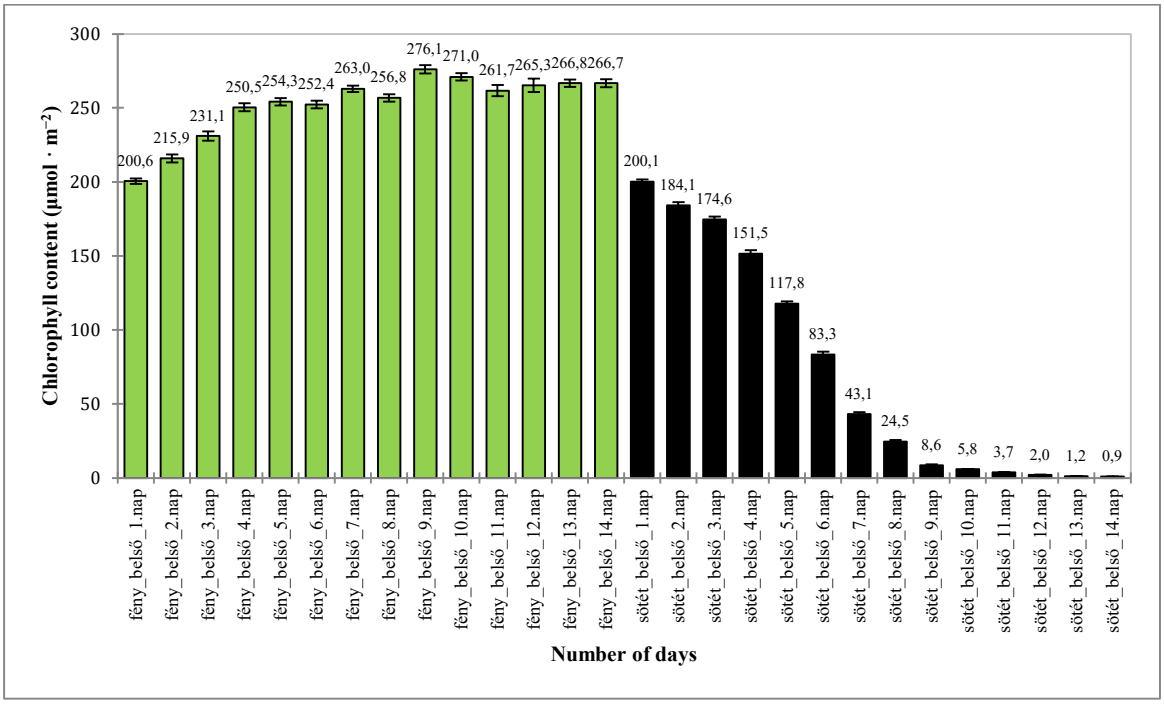

Figure 15. Changes in chlorophyll content in inner leaf of lettuce, with light treatment and in the dark, at 4°C

Changes in the chlorophyll content of lettuce leaves follow a specific pattern, and it is useful to fit a curve to the data and analyze the goodness of fit. Based on my results, it can be stated that the curve describing the change in chlorophyll content of light-treated outer ($y = 20{,}509\ln(x) + 150{,}05$; $R^2 = 0{,}8938$) and inner ($y = 26{,}607\ln(x) + 204{,}25$; $R^2 = 0{,}8985$) lettuce leaf is logarithmic, while the curve describing the change in chlorophyll content of dark-treated outer ($y = -0{,}0372x^4 + 1{,}2614x^3 - 13{,}187x^2 + 30{,}463x + 126, 93$; $R^2 = 0{,}994$) and inner ($y = 0{,}1968x^3 - 2{,}9498x^2 - 12{,}239x + 222{,}22$; $R^2 = 0{,}984$) lettuce leaves is logarithmic. polynomial curve; in all cases, the goodness of fit of the curve was very good. With my results, I proved that in the case of lettuces in an LED light environment optimized for chlorophyll content, the appropriate light conditions (photon flux, spectral characteristics) significantly contribute to the maintenance of chlorophyll content.

4.5. Color masking of green and black tea brews

4.5.1. Results of instrumental color measurement of green tea infusions

The transmission curves of the green tea infusions were very similar. It can be seen that light was transmitted starting at approximately 470 nm, while at lower wavelengths less or not at all. I made all the tea infusions from leaf tea, except for the Japanese Matcha Jikagise tea, which is commercially available as a ground tea. This infusion differed significantly from the infusions made from leaves due to the ground, powdered nature of the tea, which was reflected in its opacity and bright light green color, and its transmission value did not exceed 3%. The spectra typically run side by side, almost parallel to each other, but there were spectral crossings. The Gyokuroh gokoh tea infusion crosses the spectra of two tea infusions, while the Qing Zhen infusion crosses the spectra of another tea infusion (Figure 16).

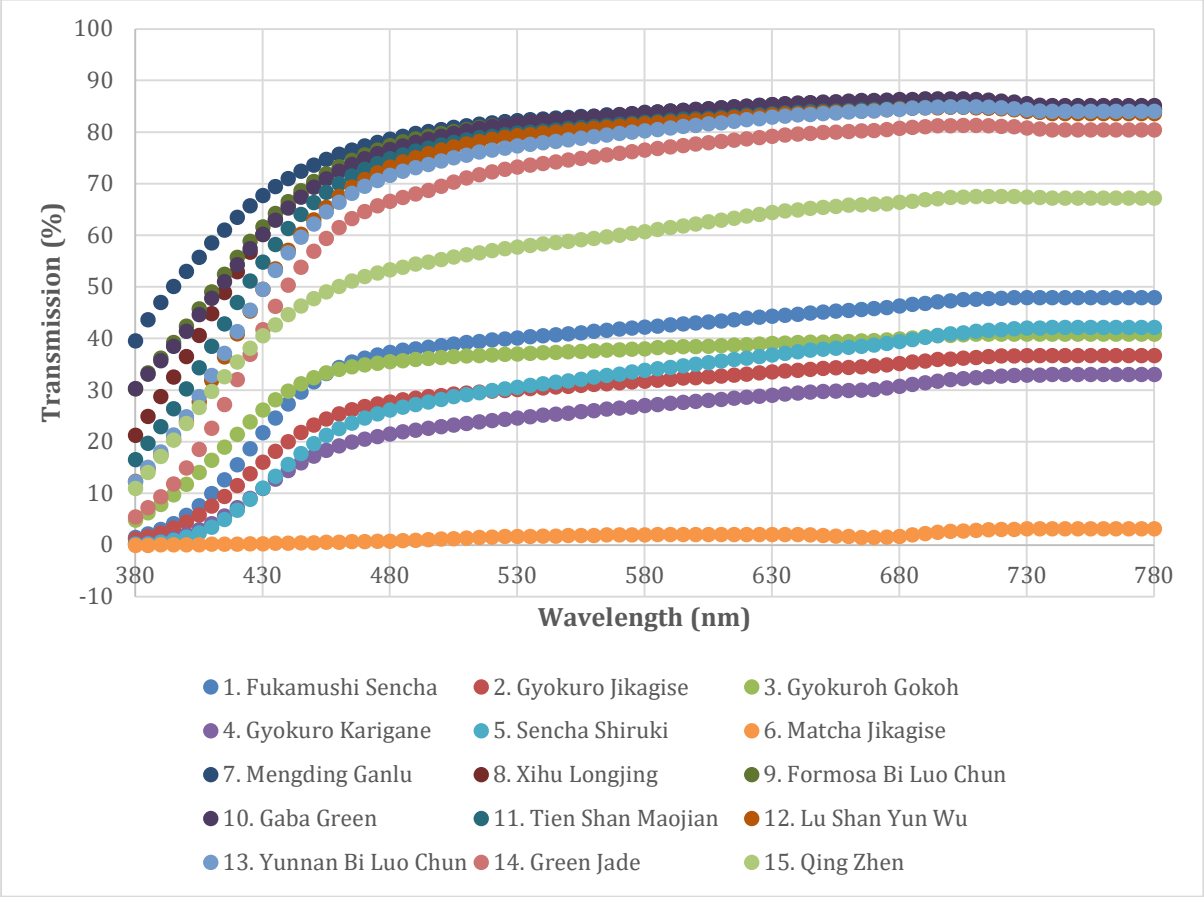

Figure 16. Transmission spectra of green tea infusions (380–780 nm)

Evaluating the L* lightness coordinate (from black to white, 0–100), it can be stated that Matcha Jikagise had the lowest value (13.8) among the samples, the second group included lighter teas (Fukamushi Sencha, Gyokuro Jikagise, Gyokuroh Gokoh, Gyokuro Karigane, Sencha Shiruki), while the third group included the lightest teas (Mengding Ganlu, Xihu Longjing, Formosa Bi Luo Chun, Gaba Green, Tien Shan Maojian, Lu Shan Yun Wu, Yunnan Bi Luo Chun, Green Jade, Qing Zhen). The a* color coordinate axis runs from red (positive values) to green (negative values), the tea samples had a small negative value, so they were slightly green in color. The b* color coordinate axis runs from yellow (positive) to blue (negative), based on the results it can be stated that the brews have a yellowish hue. The b* value was overall more heterogeneous than the a* value. Based on the C^*_{ab} saturation value, it can be concluded that the samples have low saturation, as all were less than 21. Based on the h^*_{ab} hue value, it can be concluded that all samples fell between 1.6 and 1.9 (Figure 17).

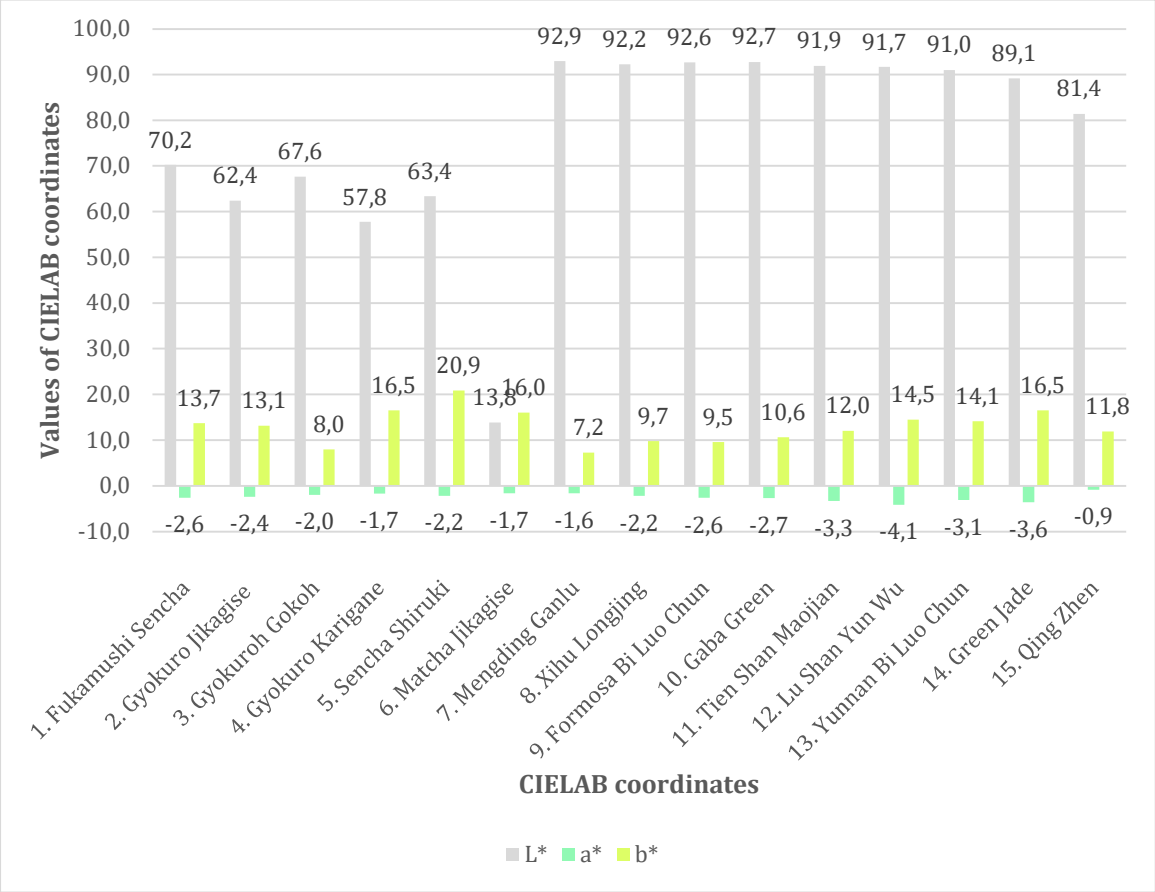

Figure 17. Graphs of color coordinates of green tea brews (L*, a*, b*)

The color coordinates of each green tea brew are presented in coordinate pairs: a*–b*, L*–a*, L*–b*. The color differences between the samples were determined in the CIELAB color space.

4.5.2. Results of instrumental color measurement of black tea brews

Based on the transmission spectra, black tea brews were more diverse than green tea brews, with lower light transmission at shorter wavelengths, while their transmittance gradually increased at longer wavelengths. Almost all curves were S-shaped, with saturation towards longer wavelengths, except for the transmittance curve of Bai Un Gongfu tea brew, which had a characteristic starting with a ramp-up phase and ending in saturation. It can be stated that in the case of black teas, the color stimuli are characterized by greater diversity, and the spectral lines intersect each other in several places (Figure 18).

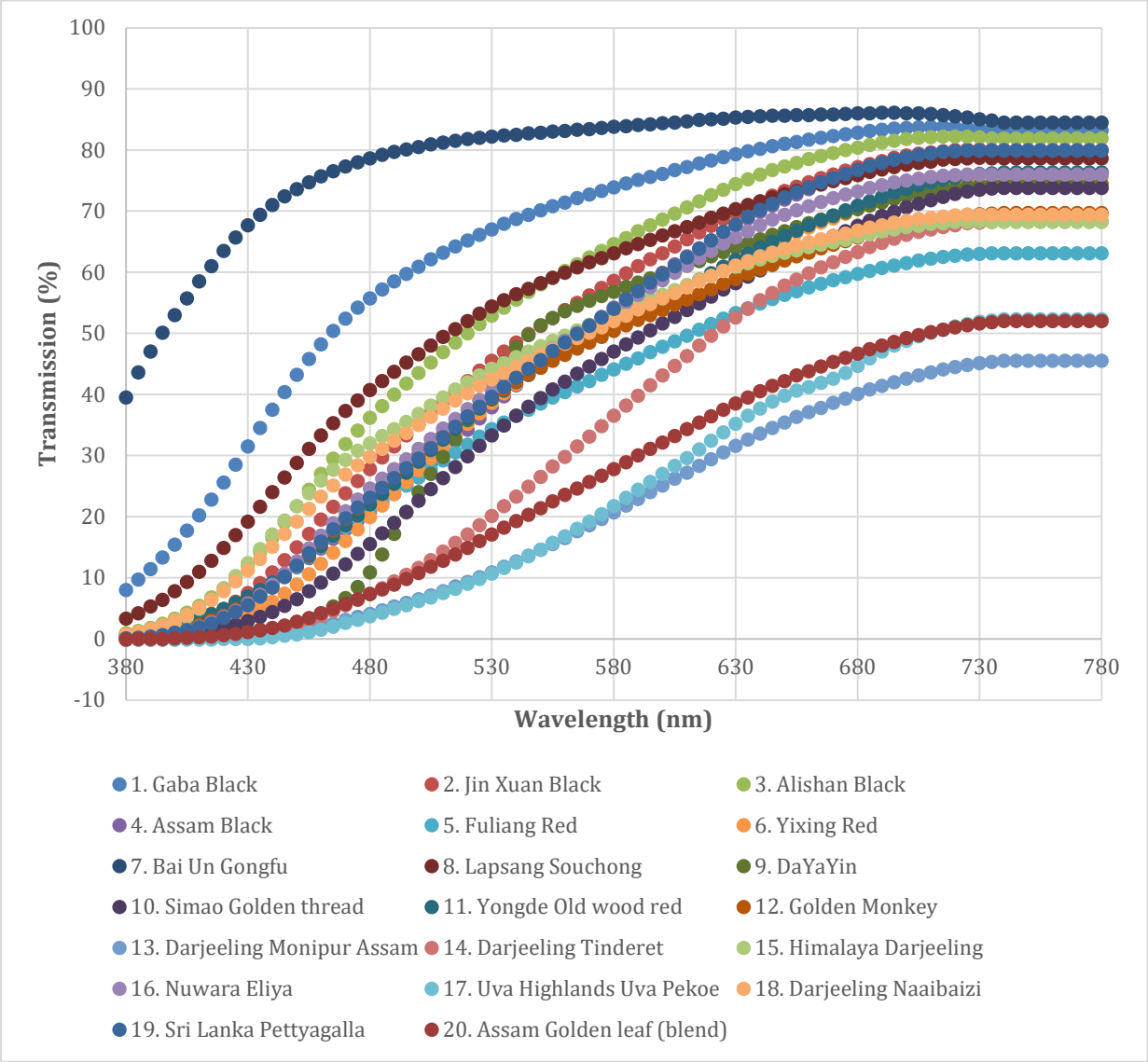

Figure 18. Transmission spectra of black tea infusions (380–780 nm)

The L* lightness coordinate (from black to white, 0–100) shows that the samples are rather light, with a wide range of values (from 47 to 93). The darkest was the Darjeeling Monipur Assam brew (47.70), the lightest was the Bai Un Gongfu brew (92.92), and all other tea brews were in between. The a* color coordinate axis runs from red (positive values) to green (negative values), and tea samples are typically characterized by reddish values. It is worth noting that the name black tea refers to the tea plant, and in Mandarin, black tea (红茶, hóng chá) is called red tea due to the reddish nature of the brew. The b* color coordinate axis extends from yellow (positive) to blue (negative), and the results show that the brews range from slightly yellowish to strongly yellowish in color, with a wide range (7–79). The C^*_{ab} saturation value indicates that the samples are more saturated than the green tea brews. The h^*_{ab} hue value indicates that all samples fall between 1.26 and 1.79. Among the black tea brews, Bai Un Gongfu differs from the others in several ways, being the lightest (L* = 92.92), the a* value on the border between red and green (a* = −1.63), the b* value with the least yellowish hue (b* = 7.24) and the lowest saturation

(C^*_{ab} = 7.42) (Figure 19).

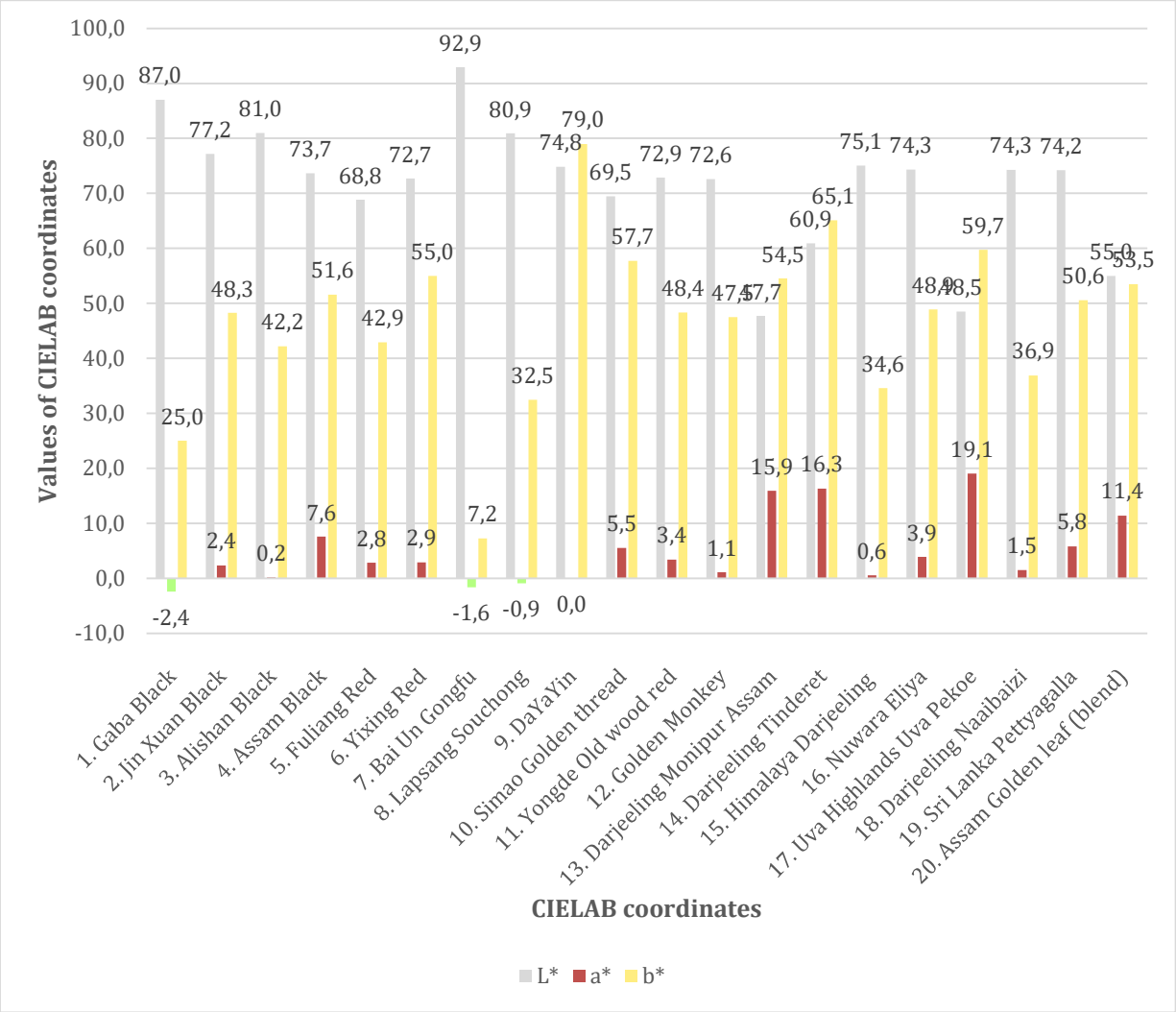

Figure 19. Graphs of color coordinates of black tea brews (L*, a*, b*)

The color coordinates of each black tea brew are presented in coordinate pairs: a*–b*, L*–a*, L*–b*. The color differences between the samples were determined in the CIELAB color space. (ΔE^*_{ab}).

4.5.3. Results of sensory tests of green tea infusions

As a first step, I tested the color vision of the 27 judges involved in the study so that only judges with normal vision would participate in the sensory tests of the samples. All the sensory judges participating in the experiment had normal vision, so they could all participate in the further sensory tests. I conducted sensory comparisons of the tea brews in a standard light booth (Pantone Color Viewing Light, D65). The tea brews prepared in the standard way were tested under standard lighting and testing conditions, using a standard tea testing cup (ISO 3103:2019), using the triangle test method, in which the judges' task was to mark the different one from a trio of tea brews containing two identical and one different samples and justify their choice (ISO 4120:2021).

In the case of green tea infusions, under D65 illumination, there was a difference between the following sample pairs: Sencha Shiruki (5)–Green Jade (14), Tien Shan Maojian (11)–Green Jade (14), Gyokuro Karigane (4)–Mengding Ganlu (7), Gyokuroh Gokoh (3)–Formosa Bi Luo Chun (9), Fukamushi Sencha (1)–Gaba Green (10). Based on the sequential (graphical) evaluation, the number of all correct answers fell above the rejection limit line. According to the result of the binomial procedure, the calculated probability value fell below the specified significance level (α = 0,05) therefore, rejecting H_0, we can state with a 95% probability that there was a statistically verifiable sensory difference between the two samples in the case of normal-sighted reviewers.

In the spectrally tunable LED light booth, I set up different masking illuminations and examined the effect of the masking lights using the triangle test method described above. Only those sample pairs that showed

differences under the standard white light source (D65) were tested under the masking light. Perfect masking means that the differences between the samples were masked in both hue and brightness. This was achieved with the Sencha Shiruki (5)–Green Jade (14) sample pair using setting 2 (red: 255, green: 0, blue: 0, white: 0, amber: 45). Based on the sequential evaluation, the number of correct answers fell below the acceptance limit. According to the result of the binomial procedure, the calculated probability value (p-value) was above the specified significance level ($\alpha = 0.05$), therefore we accept H_0, i.e. it can be stated with 95% probability that there was no statistically verifiable sensory difference between the two tea samples for normal-sighted reviewers. Setting 1 (red: 110, green: 0, blue: 0, white: 0, amber: 160) and setting 3 (red: 155, green: 0, blue: 55, white: 0, amber: 65) partially masked the differences in the Sencha Shiruki (5)–Green Jade (14) and Tien Shan Maojian (11)–Green Jade (14) sample pairs. In the triangle test, at a 95% significance level, at least 14 incorrect responses out of 27 trials are required for the masking settings to be acceptable, which in this case means that the judge incorrectly selects the different sample(s) (Table 5).

Table 5. Characterization of the masking efficiency of green teas using incorrect answers (with masking settings)

Sample Pairs (serial number)	**Number of incorrect answers**					
	D65	**1. setting 110-0-0-0-160***	**2. setting 255-0-0-0-45**	**3. setting 155-0-55-0-65**	**4. setting 205-25-25-0-0**	**5. setting 90-120-230-255-90**
Sencha Shiruki (5) Green Jade (14)	3 pcs	12 pcs	24 pcs**	9 pcs	9 pcs	3 pcs
Tien Shan Maojian (11) Green Jade (14)	3 pcs	12 pcs	9 pcs	9 pcs	12 pcs	3 pcs
Gyokuro Karigane (4) Mengding Ganlu (7)	0 pcs	0 pcs	3 pcs	3 pcs	0 pcs	0 pcs
Gyokuroh Gokoh (3) Formosa Bi Luo Chun (9)	0 pcs	0 pcs	6 pcs	0 pcs	0 pcs	0 pcs
Fukamushi Sencha (1) Gaba Green (10)	0 pcs	3 pcs	3 pcs	0 pcs	0 pcs	0 pcs

* The setting order of the masking lights applied to green tea brews is red, green, blue, white, amber

** The effect of masking is significant at the 95% significance level

4.5.4. Results of sensory tests of black tea brews

I presented the results of the color vision testing of the sensory judges participating in the study for green teas (all 27 judges proved to be normal-sighted). The sensory tests of the black tea samples were preceded by the color vision test described for green teas. I tested the black tea brews under the same conditions, in a standard light booth, under D65 illumination. After that, I examined the effects of different masking illuminations, so I performed triangle tests of the sample pairs in different masking light environments. While in the case of green teas I used several LED channels to create the illumination, in the case of black teas it seemed sufficient to use the LED spectrums separately, therefore I used red, green, blue and amber LEDs for masking. In the case of black teas, the following sample pairs showed differences in standard D65 lighting conditions: Yongde Old wood red (11)–Himalaya Darjeeling (15), Alishan Black (3)–Assam Black (4), Jin Xuan Black (2)–Golden Monkey (12), Gaba Black (1)–DaYaYin (9), Bai Lin Gongfu (7)–Sri Lanka Pettyagalla (19), Darjeeling Tinderet (14)–Assam Golden leaf (blend) (20). Based on the sequential (graphical) evaluation, the number of correct answers fell above the rejection limit. According to the result of the binomial procedure, the calculated probability value (p-value) was below the specified significance level ($\alpha = 0.05$), therefore, rejecting H0, we can state with a 95% probability that there was a statistically verifiable sensory difference between the two samples in the case of sighted judges. In the triangle test, at least 14 incorrect answers out of 27 trials are required for the masking settings to be acceptable at a 95% significance level, which means that the judge incorrectly selects the different sample(s). Perfect masking was achieved with monochromatic blue LED illumination (blue: 255) for the Darjeeling Tinderet (14)–Assam Golden leaf (blend) (20) sample pair. Perfect masking was achieved with monochromatic red LED illumination

(red: 255) for the Alishan Black (3)–Assam Black (4) sample pair. These were confirmed by the sequential evaluation and the binomial theorem evaluation results. The Darjeeling Tinderet (14)–Assam Golden leaf (blend) (20) tea brew pair is close to each other in terms of color stimulus perception, with errors occurring in all color environments. Differences due to brightness remained detectable. The research results highlighted that if the color stimulus difference between the samples is significant, the masking effect cannot be achieved. Partial masking may result from the fact that not only color masking but also luminance masking is required (Table 6).

Table 6. Characterization of the effectiveness of masking black tea using incorrect answers (with masking settings)

Sample Pairs (serial number)	Number of incorrect answers			
	1. setting red LED 255	2. setting green LED 255	3. setting blue LED 255	4. setting amber LED 255
Yongde Old wood red (11) Himalaya Darjeeling (15)	0 pcs	0 pcs	0 pcs	0 pcs
Alishan Black (3) Assam Black (4)	15 pcs*	0 pcs	0 pcs	3 pcs
Jin Xuan Black (2) Golden Monkey (12)	0 pcs	0 pcs	3 pcs	9 pcs
Gaba Black (1) DaYaYin (9)	0 pcs	0 pcs	0 pcs	0 pcs
Bai Lin Gongfu (7) Sri Lanka Pettyagalla (19)	3 pcs	0 pcs	0 pcs	12 pcs
Darjeeling Tinderet (14) Assam Golden leaf (blend) (20)	12 pcs	3 pcs	18 pcs*	12 pcs

* The effect of masking is significant at the 95% significance level

In summary, it can be stated that in the case of tea beverages, by color masking and determining spectral characteristics, the differences between certain pairs of samples with different color stimuli can be partially or completely masked, in the case of normal-sighted judges. Thanks to this, under perfect masking illumination, the expectation errors resulting from perception do not distort the judgment of other sensory characteristics of tea beverages (aroma, taste, texture and mouthfeel).

4.6. Masking of sunflower cooking oils, rapeseed cooking oils and blended cooking oils with a standard colored olive oil test cup

4.6.1. Results of instrumental color measurement of sunflower edible oils, rapeseed edible oils and blended edible oils

To characterize the spectral properties of sunflower edible oils, rapeseed edible oils, and blended edible oils, I determined the characteristics of the spectra. The curves were similar in nature, with intensively increasing absorption in the 380–480 nm wavelength range and slow saturation from 480 nm to 780 nm. The spectral curves of the samples are typically close to each other, with Rapso 100% rapeseed edible oil (sample 9) having a lower, and Natur Organic sunflower edible oil (sample 8) having a higher transmission value than the other samples (Figure 20).

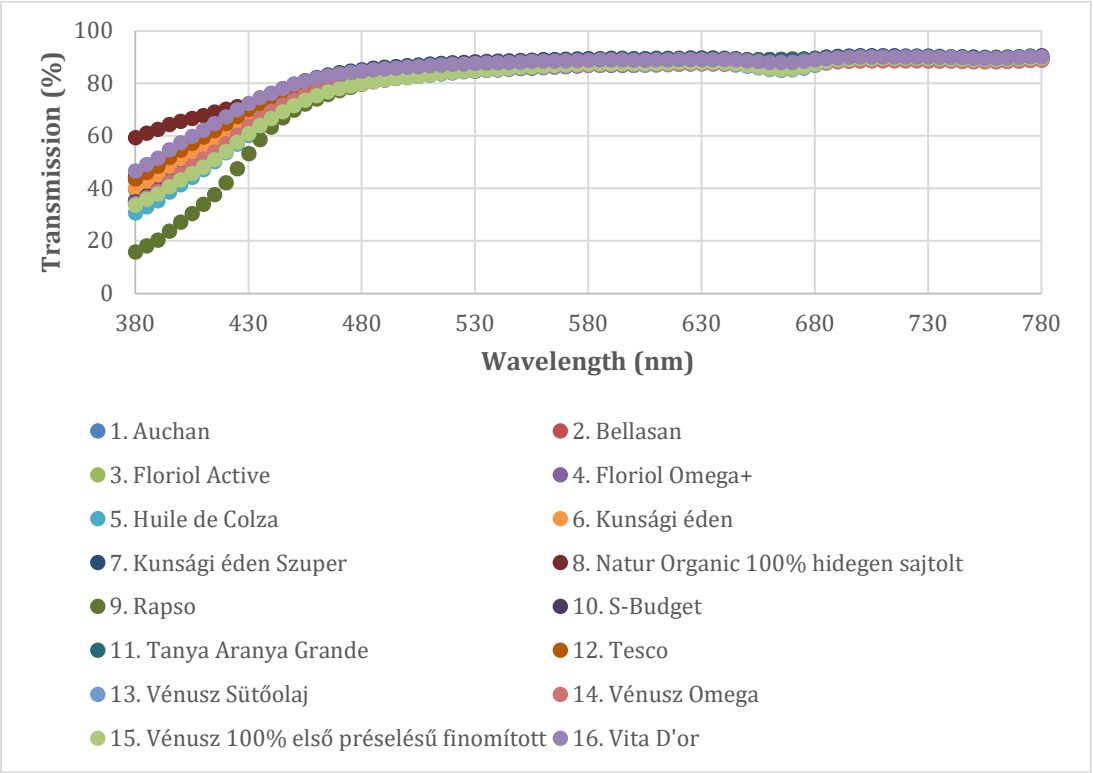

Figure 20. Transmission spectra of cooking oil samples (380–780 nm)

I calculated the coordinates defined in the CIELAB color space from the transmission curves of the cooking oil samples (L*, a*, b*, C^*_{ab}, h^*_{ab}) (Table 7).

Table 7. CIELAB color coordinates (L*, a*, b*, C^*_{ab}, h^*_{ab}) of sunflower oil, rapeseed oil, and blended oil samples. (I have marked 100% rapeseed oils and their color coordinate values in bold.)

No.	Trade name	Composition	L*	a*	b*	C^*_{ab}	h^*_{ab}
1.	Auchan	refined sunflower	94,37	−2,22	7,13	7,47	1,87
2.	Bellasan	refined sunflower	94,23	−2,88	9,44	9,87	1,87
3.	**Floriol Active**	**refined rapeseed**	**94,87**	**−2,76**	**7,76**	**8,24**	**1,91**
4.	Floriol Omega+	refined rapeseed (70%) high oleic sunflower (30%)	94,87	−2,77	7,80	8,28	1,91
5.	**Huile de Colza (Auchan budget)**	**refined rapeseed**	**94,63**	**−4,35**	**11,96**	**12,72**	**1,92**
6.	Kunsági éden	refined sunflower	94,50	−2,60	8,09	8,49	1,88
7.	Kunsági éden Szuper	refined sunflower (70%) high oleic refined sunflower (15%) refined rapeseed (15%)	95,35	−2,43	6,94	7,36	1,91
8.	Natur Organic 100% hidegen sajtolt	cold pressed sunflower seeds from peeled husks	94,91	−2,55	8,03	8,43	1,88
9.	**Rapso**	**refined rapeseed**	**94,58**	**−5,00**	**14,33**	**15,18**	**1,91**
10.	S-Budget	refined sunflower	93,99	−3,20	10,52	10,99	1,87
11.	Tanya Aranya Grande	refined sunflower	94,87	−2,29	7,49	7,83	1,87
12.	Tesco	refined sunflower	94,68	−2,36	7,30	7,67	1,88
13.	Vénusz Sütőolaj	first pressed sunflower (85%) high oleic sunflower (15%)	94,00	−3,10	10,13	10,60	1,87
14.	Vénusz Omega	refined rapeseed (60%) first pressed refined sunflower (40%)	94,20	−3,16	9,69	10,20	1,89
15.	Vénusz 100% első préselésű finomított	first pressed refined sunflower oil	94,14	−3,33	11,17	11,66	1,86
16.	Vita D'or	sunflower	95,10	−2,21	6,51	6,87	1,90

By evaluating the L* lightness coordinate (from black to white, 0–100), it can be stated that the cooking oil samples are uniformly light, have high light transmittance, are clear, and the range of lightness values of the samples is small (L* = 94.0–95.5). Based on the a* color coordinate values, the cooking oils showed greater variability and were slightly green in color (a* = −5.0–(−0.3)). Based on the b* color coordinate values, the cooking oils showed the greatest variability, from very slightly yellowish to yellow (b* = 6.51–14.3). Based on the C^*_{ab} saturation value, it can be stated that the samples have low color saturation (C^*_{ab} = 6.87–15.5). Based on the h^*_{ab} hue value, it can be stated that all samples fell between 1.6 and 1.9 (Figure 21).

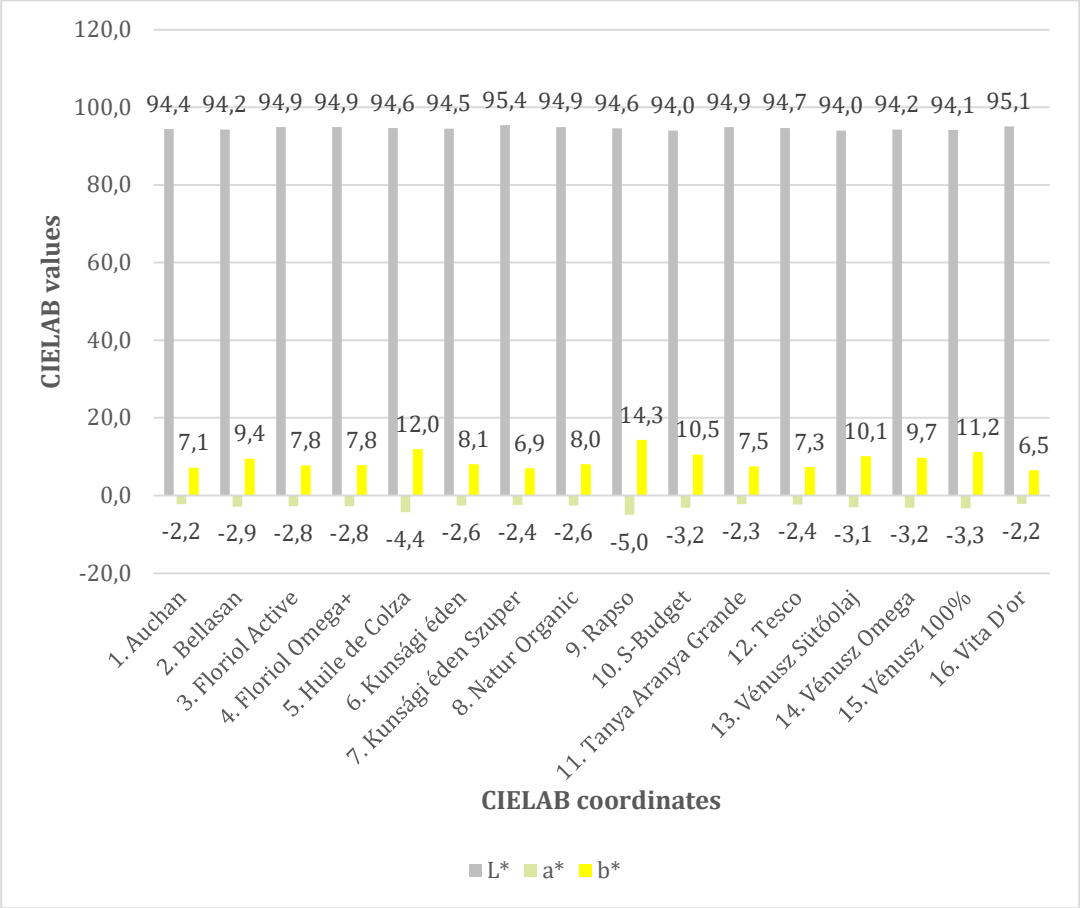

Figure 21. Graphs of the color coordinates of cooking oil samples (L*, a*, b*)

The color coordinates of each cooking oil sample are presented in coordinate pairs: a*–b*, L*–a*, L*–b*. The color differences between the samples were determined in the CIELAB color space (ΔE^*_{ab}). Based on the color differences determined by instrumental measurements, the cooking oil samples differed from each other to varying degrees. I present my results based on the perceptible difference threshold (ΔE^*_{ab}) and their categories: no difference ($\Delta E^*_{ab} = 0$): no such sample pair; not perceptible ($\Delta E^*_{ab} \leq 0.5$): 9 sample pairs; barely perceptible ($0.5 < \Delta E^*_{ab} \leq 1.5$): 35 sample pairs; perceptible ($1.5 < \Delta E^*_{ab} \leq 3.0$): 31 sample pairs; visible ($3.0 < \Delta E^*_{ab} \leq 6.0$): 36 sample pairs; large difference ($6.0 < \Delta E^*_{ab}$): 9 sample pairs (Mokrzycki & Tatol, 2011). The samples included sunflower edible oils, rapeseed edible oils and blended edible oils. The differences between the samples cannot be explained by the lightness (L*) value, as the samples showed high homogeneity in this parameter (L* = 94.0–95.5). It should be noted that rapeseed edible oils typically differed from the sunflower edible oil samples, and there were differences in the degree of difference between them. It is worth noting that two 100% rapeseed oil samples were the yellowest, most greenish, and most saturated (Rapso: b* = 14.33, a* = −5.00, C^*_{ab} = 15.18; Huile de Colza: b* = 11.96, a* = −4.35, C^*_{ab} = 12.72). The third 100% refined rapeseed oil, Floriol Active, differed from the other samples to varying degrees. Among the sunflower edible oils, Venus 100% first pressing should be highlighted, which differed with the greatest visible difference from the other sunflower edible oil and sunflower-rapeseed blend edible oil samples, as it was the yellowest, greenest and most saturated in color (b* = 11.17, a* = −3.33, C^*_{ab} = 11.66). The sunflower edible oil samples had similar parameters overall, so they differed from each

other the least, in many cases with no or barely perceptible differences. This is due to the similar values of their color coordinates (L*, a*, b*) (Table 8).

Table 8. Color difference perceptions calculated from the CIELAB L*, a*, b* coordinates of sunflower cooking oil, rapeseed cooking oil and mixed cooking oil samples

sample	01 Auchan	02 Bellasan	03 Floriol Active	04 Floriol Omega+	05 Huile de Colza	06 Kunsági Éden	07 Kunsági É. Szuper	08 Natur Organic	09 Rapso	10 S-Budget	11 Tanya Aranya	12 Tesco	13 Vénusz Sütőolaj	14 Vénusz Omega	15 Vénusz 100%	16 Vita D'or
01 Auchan	–	2,4	0,97	1	5,28	1,04	1,02	1,1	7,72	3,55	0,62	0,38	3,16	2,74	4,2	0,96
02 Bellasan	perceptible	–	1,8	1,76	2,95	1,41	2,77	1,59	5,35	1,15	2,13	2,24	0,77	0,38	1,8	3,13
03 Floriol Active	barely perceptible	perceptible	–	0,04	4,49	0,52	1,01	0,34	6,94	2,92	0,55	0,64	2,55	2,08	3,53	1,39
04 Floriol Omega+	barely perceptible	perceptible	not perceptible	–	4,45	0,49	1,04	0,32	6,91	2,89	0,57	0,67	2,51	2,04	3,5	1,43
05 Huile de Colza	visible	perceptible	visible	visible	–	4,25	5,41	4,32	2,46	1,95	4,92	5,06	2,3	2,59	1,38	5,87
06 Kunsági Éden	barely perceptible	barely perceptible	barely perceptible	not perceptible	visible	–	1,43	0,41	6,69	2,56	0,76	0,84	2,17	1,73	3,19	1,73
07 Kunsági É. Szuper	barely perceptible	perceptible	barely perceptible	barely perceptible	visible	barely perceptible	–	1,18	7,86	3,9	0,74	0,76	3,53	3,07	4,49	0,55
08 Natur Organic	barely perceptible	perceptible	not perceptible	not perceptible	visible	not perceptible	barely perceptible	–	6,76	2,73	0,6	0,79	2,36	1,9	3,32	1,58
09 Rapso	substantial difference	visible	substantial difference	substantial difference	perceptible	substantial difference	substantial difference	substantial difference	–	4,26	7,36	7,51	4,64	5	3,6	8,32
10 S-Budget	visible	barely perceptible	perceptible	perceptible	perceptible	perceptible	visible	perceptible	visible	–	3,28	3,39	0,39	0,85	0,69	4,28
11 Tanya Aranya	barely perceptible	perceptible	barely perceptible	barely perceptible	visible	barely perceptible	barely perceptible	barely perceptible	substantial difference	visible	–	0,28	2,9	2,46	3,9	1,02
12 Tesco	not perceptible	perceptible	barely perceptible	barely perceptible	visible	barely perceptible	barely perceptible	barely perceptible	substantial difference	visible	not perceptible	–	3,01	2,57	4,03	0,91
13 Vénusz Sütőolaj	visible	barely perceptible	perceptible	perceptible	perceptible	perceptible	visible	perceptible	visible	not perceptible	perceptible	visible	–	0,49	1,07	3,9
14 Vénusz Omega	perceptible	not perceptible	perceptible	perceptible	perceptible	perceptible	visible	perceptible	visible	barely perceptible	perceptible	perceptible	not perceptible	–	1,49	3,45
15 Vénusz 100%	visible	perceptible	visible	visible	barely perceptible	visible	visible	visible	visible	barely perceptible	visible	visible	barely perceptible	barely perceptible	–	4,9
16 Vita D'or	barely perceptible	visible	barely perceptible	barely perceptible	visible	perceptible	barely perceptible	perceptible	substantial difference	visible	barely perceptible	barely perceptible	visible	visible	visible	–

4.6.2. Sensory tests of sunflower edible oils, rapeseed edible oils and blended edible oils

In the first step, I tested the color vision of the 36 judges included in the study so that only normal-sighted judges would participate in the sensory tests of the samples. Of the sensory judges participating in the experiment, 32 had normal vision, while 4 men were found to be colorblind according to the Ishihara test, who also performed poorly in the Farnsworth–Munsell test: I excluded them from further sensory tests. The determination of the visual differences of the edible oils was performed in a standard light booth (Pantone Color Viewing Light, D65). Under standard lighting and testing conditions, I performed the standard sensory test of the triangle test (ISO 4120:2021, ISO 16820:2019) in a transparent olive oil test glass next to a standard white light source (D65). Based on the results, the judges could not distinguish between the following samples in a light booth, under standard white (D65) lighting: Auchan–Tesco (1–12), Bellasan–Vénusz Omega (2–14), Floriol Active–Floriol Omega+ (3–4), Floriol Active–Natur Organic (3–8), Floriol Omega+–Natur Organic (4–8), Kunsági Éden–Natur Organic (6–8), S-Budget–Vénusz Cooking Oil (10–13), Tanya Aranya Grande–Tesco (11–12), Vénusz Cooking Oil–Vénusz Omega (13–14). The sensory results confirm the results of the instrumental measurements in that no sensory difference was found as a result of the instrumental measurement in the case of the cooking oil sample pairs falling into the non-perceptible category. From the barely perceptible category, there was no sensory difference between the members of a few pairs of exclusively 100% sunflower cooking oil samples: Bellasan–S-Budget (2–10), Kunsági Éden–Tesco (6–12), Natur Organic–Tesco (8–12), Bellasan–Vénusz Sütőolaj (2–13). In the case of all other pairs of samples, there was a significant sensory difference between the cooking oil samples based on the triangle test.

5. Conclusions and recommendations

The creation of maps based on DLI values is a strategic issue, as they serve as a decision-making tool, providing an objective information base for optimizing crop production. Among other things, these maps can help in formulating recommendations for crop cultivation regarding currently cultivated or future potential varieties, and in planning temporary, regional, or crop-specific shade management systems. They also enable crop production to meet market demands more effectively, as they can help optimize conditions for early ripening, organic farming, extended production, and multiple harvests. With increasing urbanization, plant-based planning of urban green spaces is coming to the fore, where knowledge of seasonal and regional patterns of DLI values provides the basis for the right strategy. The limitation of DLI maps is that their accuracy depends on spatial resolution and data collection density. Large-scale DLI data are typically provided by meteorological stations and satellite measurements. However, the spatial distribution of meteorological stations is not always homogeneous or sufficiently dense, which means that interpolation or data replacement techniques are often necessary. These methods can affect the overall accuracy and reliability of DLI maps. It should also be noted that DLI maps provide guidance but are not a substitute for local measurements.

I explored the regional and seasonal patterns of Portugal's DLI maps, and the maps on which this is based have been completed. These may be important because the country is particularly vulnerable to the effects of global climate change and faces ongoing challenges in terms of energy efficiency and sustainability, so developing climate-resilient agriculture is a pressing task that DLI maps can support. The 5 $mol \cdot m^{-2} \cdot d^{-1}$ resolution maps provide an opportunity to compare the special regional-seasonal DLI patterns of existing maps, which also have a resolution of 5 $mol \cdot m^{-2} \cdot d^{-1}$. I have compared the DLI patterns of Portugal and Spain in my publication, and I recommend doing the same for other countries in further research. To my knowledge, DLI maps with a resolution of 5 $mol \cdot m^{-2} \cdot d^{-1}$ have been produced for China, the USA, Hungary, and Slovakia. Our research group has set itself the goal of producing DLI maps for all European countries. The automation of the data collection process required for DLI mapping, the PHP script I wrote, and its further development are a great help in achieving this goal. In addition to software development, I plan to incorporate new tools to further increase efficiency, now also on Windows and Linux operating systems. In the long term, it may also be advisable to pay attention to various machine learning methods and predictive models, which can provide higher quality results than human observations (provided that their specific limitations are properly addressed).

The validation of the light conditions in the climate chamber is key to the reliability of the results. The light source used in my research consists of several structural elements (heat sink, printed circuit board, LEDs, optical lens) and is only one of the components of the lighting system. The emitted photon flux is influenced by the combined properties of all components of the entire electronic system, while the number of photons reaching the plant surface can be modified by environmental factors in the climate chamber, such as reflection conditions or the light transmittance of the medium. In my research, I have demonstrated that identical LED light sources, with the same settings, the same light source-sample geometry, and the same light reflection environment, can produce different photon flux values. I therefore recommend that local, real-world conditions be checked with instrumental measurements during the design, implementation, and monitoring of plant lighting, with particular attention to homogeneity, distance dependence, and edge dependence of photon flux density. This is especially true if we want to optimize the light environment beyond the parameters specified by the manufacturer.

In my research, I tested the effect of LED lighting optimized for chlorophyll content and confirmed that appropriate lighting conditions (photon flux, spectral characteristics) significantly contribute to maintaining chlorophyll content. My research has demonstrated that the use of specially designed lighting environments can increase the shelf life of the salad variety studied. In further experiments, it would be advisable to implement my results in practice, for example, in retail practice by creating chlorophyll-optimized lighting environments above display counters. Overall, it can be concluded that LED lighting environments optimized for plant needs can effectively contribute to keeping plants fresh and minimizing food waste. Many varieties of the Lactuca genus

(e.g., butterhead, batavia, iceberg, romaine, curly leaf, and oak leaf lettuce) are used in horticultural crops. As consumer demands change, lettuce grown in closed systems using supplementary lighting and hydroponics are becoming increasingly popular during the winter months. However, it should be noted that when stored on store shelves or in refrigerators, significant water loss typically occurs after a few days, accompanied by a significant deterioration in nutritional parameters.

In my research, I tested two sensory visual masking methods. In the first case, I examined different illuminations that can be produced in a spectrally tunable LED light cabin, in terms of masking the color differences between green and black tea infusions. In the second case, I adapted a standard colored olive oil test cup to mask the color differences between sunflower, rapeseed, and blended cooking oil samples. During masking with light environments, I verified that there is a light environment in which the judges can no longer distinguish between the green and black tea infusion sample pairs, while in a light environment that follows the spectral distribution of natural sunlight (D65), the same green and black tea sample pairs were significantly different to the judges. The characteristics of the spectra of green teas consisted of a series of curves that were more similar to each other than to the transmittance curves of black teas. The transmission curves of green teas generally differed in terms of light transmission but were almost parallel. In the case of black teas, however, there was more variation between the color samples, and the spectra crossed each other. In further research, I plan to investigate the masking possibilities of other tea infusions with different degrees of fermentation and origins (yellow, white, oolong, pu-erh) by testing spectrally tunable light cabin masking environments.

I tested sunflower oils, rapeseed oils, and blended oils using color masking with colored cobalt blue test cups. I did not test further in masking cups those pairs of edible oil samples that did not show significant differences between samples under standard conditions and in transparent cups. For the remaining sample pairs, I obtained results indicating successful masking: in standard, colored (cobalt blue) olive oil testing glasses, there was no significant ($\alpha = 0,05$) sensory difference between the samples in any of the sample pairs. The masking effect of the cup is due, on the one hand, to its light-reducing (darkening) effect and, on the other hand, to its spectral color filtering effect.

6. New scientific results

1. In my research, I was the first to create maps of continental Portugal based on daily light integral (DLI, $mol \cdot m^{-2} \cdot d^{-1}$) values, which show the monthly breakdown of the daily light integral, i.e., the integrals of the photon flux values measured per second during one day in the photosynthetically active radiation wavelength range (400–700 nm). I created spatial visualizations of DLI values for continental Portugal in monthly breakdowns, in two different resolutions (2 $mol \cdot m^{-2} \cdot d^{-1}$, 5 $mol \cdot m^{-2} \cdot d^{-1}$). The highly detailed 2 $mol \cdot m^{-2} \cdot d^{-1}$ map was created to identify regional differences, while the 5 $mol \cdot m^{-2} \cdot d^{-1}$ map was created for continental-scale comparability with existing DLI maps. In my research, I was the first to reveal the characteristic regional and seasonal patterns.

2. In my research, I automated the data collection workflow required for DLI mapping. By developing a program written in the PHP (Hypertext Preprocessor) scripting language, I developed a database-based storage method (MySQL) that is several orders of magnitude faster, more efficient, and easier to control. By developing the script and adding a self-correcting mechanism, I increased the reliability of data collection, increased the level of automation, and reduced the need for supervision. The formal error rate is zero when using the script.

3. In my experiments, I have demonstrated that identical LED light sources, with the same settings, the same light source pattern geometry, and the same light reflection environment, can produce different photon flux values due to differences in the structural components of the light sources (heat sink, printed circuit board, LEDs, optical lens) and the associated electronic systems (power supply, control electronics, cables). In my experiments, I have verified that the closer the test surface is to the light source, the greater the difference in light flux between the two chambers at the same point: 0–50% difference (155 mm), 5–25% difference (245 mm), 4–18% difference (335 mm).

4. In my research, I demonstrated that specially designed lighting environments can increase the chlorophyll content of Lactuca sativa 'Casey' in an environment that stimulates chlorophyll production, with a photosynthetic photon flux density of 150 $\mu mol \cdot m^{-2} \cdot s^{-1}$, in the wavelength range of 400–750 nm, with LED lighting, a 10-minute light/10-minute dark light program, at a temperature of 4°C and 70% relative humidity. I verified that the chlorophyll content of both the light-treated outer leaves and the light-treated inner leaves significantly ($\alpha = 0,05$) exceeded the chlorophyll content of the lettuce leaves kept in the dark from day 9 onwards. I was the first to characterize that, under the applied light treatment and conditions, the curve describing the chlorophyll content of the light-treated outer and inner lettuce leaves is logarithmic. The goodness of fit of the curves was very good in both cases (external leaves: $R^2 = 0.8938$, internal leaves: $R^2 = 0.8985$).

5. In my research, I used sensory tests to prove that the LED combination (red (640 nm, 100%) and amber (590 nm, 17.64%)) is suitable for masking color differences in green tea samples (Sencha Shiruki–Green Jade) made from fermented leaves of the tea plant (Camellia sinensis L.). In my research, I also demonstrated through sensory tests that the monochromatic red (640 nm, 100%) LED light environment is suitable for masking the color differences between a sample pair of black tea brews made from the fermented leaves of the tea plant (*Camellia sinensis* L.) (Alishan Black–Assam Black), while the monochromatic blue (460 nm, 100%) LED light environment is suitable for masking the color differences of another sample pair (Darjeeling Tinderet–Assam Golden leaf).

6. In my research, I used sensory tests to prove that cobalt blue olive oil test cups are suitable for use with a standard white light source (D65) to visually distinguish between sunflower oils, rapeseed oils, and mixed edible oils in transparent olive oil test cups, which were examined during sensory tests. rapeseed oils, and mixed cooking oils, which were visually distinguishable from each other during the sensory tests. In my research, I spectrally characterized the tested cooking oil samples and the colored (cobalt blue) standard test cup developed for olive oils.

7. List of publications in the field of studies

Book chapter

Urbin, Á., Nagy, B. V., Nyitrai, Á., **Szabó, D.**, Sipos, L. Színkülönbségek maszkolása érzékszervi vizsgálatokban. In: Nagy, János (2022): Világítástechnikai évkönyv 2020-2021. pp. 40-43.

Articles

Szabó, D., Jung, A., Varga, Z., Hajdú, E., Revoly, A., Lausch, A., Vohland, M., & Sipos, L. (2025). Agricultural Lighting Strategies in Portugal: Insights from DLI Mapping. Agronomy, 15(12), 2860. https://doi.org/10.3390/agronomy15122860. (Q1, IF: 3,4)

Jung, A., **Szabó, D.**, Varga, Z., Lausch, A., Vohland, M., & Sipos, L. (2024b). Daily light integral maps for agriculture lighting design in Spain. *Smart Agricultural Technology*, *9*, 100681. https://doi.org/10.1016/j.atech.2024.100681. (Q1, IF: 5,7)

Jung, A., **Szabó, D.**, Varga, Z., Pék, Z., Vohland, M., & Sipos, L. (2024a). Spatially scaled and customised daily light integral maps for horticulture lighting design. *NJAS: Impact in Agricultural and Life Sciences*, *96*(1), 2349522. https://doi.org/10.1080/27685241.2024.2349522. (Q2, IF: 2,6)

Sipos, L., Nyitrai, A., **Szabo, D.**, Urbin, A., & Nagy, B. V. (2021). Former and potential developments in sensory color masking–Review. Trends in Food Science & Technology, 111, 1-11. (D1, IF: 12,563)

Bodor, Z., Benedek, C., Urbin, Á., **Szabó, D.**, & Sipos, L. (2021). Colour of honey: can we trust the Pfund scale?–An alternative graphical tool covering the whole visible spectra. *LWT*, *149*, 111859. (D1, IF: 5,85)

Sipos, L., Nyitrai, Á., **Szabó, D.**, Dominek, M., Urbin, Á., & Nagy, B. V. (2020). Zöld és fekete tea (*Camellia sinensis* L.) főzeteire specifikált színelmaszkolási rendszer érzékszervi validálása. Élelmiszervizsgálati Közlemények, 66(1), 2830-2844. (Q4)

Sipos, L., Nyitrai, Á., **Szabó, D.**, Urbin, Á., & Nagy, B. V. (2020). Vision tests of sensory judges-review (Érzékszervi bírálók látásvizsgálati tesztjei-áttekintés). Élelmiszervizsgálati Közlemények, 66(4), 3202-3218. (Q4)

Conference abstracts

Szabó Dániel, Jung András, Varga Zsófia, Hajdú Edina, Revoly András, Angela Lausch, Michael Vohland, Sipos László. Portugália napi fényintegrál térképeinek fejlesztése. In: Nyitrainé, Sárdy Diána Ágnes; Kókai, Zoltán; Bodor-Pesti, Péter; Deák, Tamás (szerk.) A 2025. évi Lippay János – Ormos Imre – Vas Károly (LOV) Tudományos Ülés összefoglalói. Budapest, Magyarország : Magyar Agrár- és Élettudományi Egyetem, Budai Campus (2025) 87 p. pp. 33-33. , 1 p.

Szabó Dániel, Urbin Ágnes, Sipos László. Fodros saláta (*Lactuca sativa* var. *crispa*) pulton tarthatósági idejének növelése LED fényforrású klímakamrában. In: Nyitrainé, Sárdy Diána Ágnes; Kókai, Zoltán; Bodor-Pesti, Péter; Deák, Tamás (szerk.) A 2025. évi Lippay János – Ormos Imre – Vas Károly (LOV) Tudományos Ülés összefoglalói. Budapest, Magyarország : Magyar Agrár- és Élettudományi Egyetem, Budai Campus (2025) 87 p. pp. 80-80. , 1 p.

Szabó Dániel, Csuja Zoltán, Dombi Zoltán, Bozóki Sándor, Urbin Ágnes, Sipos László. Olívaolajok színmaszkolásának lehetőségei az érzékszervi kutatásokban. In: Fodor, Marietta; Bodor-Pesti, Péter; Deák, Tamás (szerk.) A 2023. évi Lippay János – Ormos Imre – Vas Károly (LOV) Tudományos Ülésszak összefoglalói Abstracts of János Lippay – Imre Ormos – Károly Vas (LOV) Scientific Meeting, 2023. Budapest, Magyarország : Magyar Agrár- és Élettudományi Egyetem, Budai Campus (2024) 149 p. pp. 130-131. , 2 p.

Sipos László, **Szabó Dániel**, Urbin Ágnes. Színmaszkolás megoldásai és trendjei az érzékszervi kutatásokban. In: Hungalimentaria 2023 Konferencia, „Élelmiszer-biztonság folyton változó környezetben". (2023) p. 33804965

Szabó Dániel, Urbin Ágnes, Sipos László. Colour-masking of domestic paprika (Capsicum annuum L.) powder. In: Gyalai, Ingrid; Czóbel, Szilárd (szerk.) 20th Wellmann International Scientific Conference : Hódmezővásárhely, 3rd April 2023. Hódmezővásárhely, Magyarország : University of Szeged Faculty of Agriculture (2023) 97 p. pp. 11-11. , 1 p.

Szabó Dániel, Urbin Ágnes, Nagy Balázs Vince, Sipos László. Good practice of colour masking in sensory research. In: Szalóki-Dorkó, Lilla; Batáné Vidács, Ildikó; Kumar, Pradeep; Pomázi, Andrea; Gere, Attila (szerk.) 4th FoodConf - International Conference on Food Science and Technology. Book of Abstracts. Bicske, Magyarország : Élelmiszertudományért OKF Alapítvány (2022) pp. 98-98. , 1 p.

Sipos László, **Szabó Dániel**, Nyitrai Ákos, Urbin Ágnes, Nagy Balázs Vince. Érzékszervi bírálók látásvizsgálatai és élelmiszerek színmaszkolása. In: WESSLING, Hungary Kft. WESSLING Hungary Kft. Hungalimentaria 2021 - online konferencia: Állami és magán laboratóriumok együtt az élelmiszerbiztonságért. (2021). Budapest, Magyarország : WESSLING Hungary Kft. (2021) pp. 37-37. , 1 p.

Sipos László, Nyitrai Ákos, **Szabó Dániel**, Urbin Ágnes, Nagy Balázs Vince. Spektrálisan szabályozható érzékszervi maszkoló-rendszer fejlesztése. In: Fodor, Marietta; Bodor, Péter (szerk.) SZIENtific meeting for young researchers - Ifjú Tehetségek Találkozója (ITT). Gödöllő, Magyarország : Szent István University (2019) 353 p. pp. 237-249. , 13 p.

References

Domestic and international standards

IOC (2018): International Olive Council. Sensory Analysis of Olive Oil: Method for the Organoleptic Assessment of Virgin Olive Oil. COI/T.20/Doc. No 15/Rev 10, 2018.

IOC (2020a): International Olive Council. Sensory Analysis of Olive Oil: Standard Glass For Oil Tasting. COI/T.20/Doc. No 5/Rev 2, 2020.

ISO 16657:2023 Sensory analysis — Apparatus — Olive oil tasting glass

ISO 16820:2019 Sensory analysis — Methodology — Sequential analysis

ISO 3103:2019 Tea — Preparation of liquor for use in sensory tests.

ISO 4120:2021 Sensory analysis — Methodology — Triangle test

Scientific publications

Fraga, H., & Santos, J. A. (2021). Assessment of climate change impacts on chilling and forcing for the main fresh fruit regions in Portugal. Frontiers in plant science, 12, 689121. https://doi.org/10.3389/fpls.2021.689121

Mokrzycki, W. S., & Tatol, M. (2011). Colour differenceΔ EA survey. Mach. Graph. Vis, 20(4), 383-411.

Pereira, S. C., Carvalho, D., & Rocha, A. (2021). Temperature and precipitation extremes over the Iberian Peninsula under climate change scenarios: A review. Climate, 9(9), 139. https://doi.org/10.3390/cli9090139

Sources of images used in figures

I1 http://www.aoesh.com/index.php/product/index/g/e/id/25.html